PD-1 Suppresses the Osteogenic and Odontogenic Differentiation of Stem Cells From Dental Apical Papilla via Targeting SHP2/NF-κB axis

Na Li
 Nanjing Medical University

Zehan Li
 Nanjing Medical University

Lin Fu
 Nanjing Medical University

Ming Yan
 Nanjing Medical University

Yanqiu Wang
 Nanjing Medical University

Jinhua Yu (✉ yujinhua@njmu.edu.cn)
 Nanjing Medical University   https://orcid.org/0000-0003-4874-9910

Jintao Wu
 Nanjing Medical University

Research

Abstract

Background

Stem cells from the apical papilla (SCAPs) are important for tooth root development and regeneration of root dentin. Here, we examined the expression of programmed cell death protein-1 (PD-1) in SCAPs and investigated the effect of PD-1 on odontogenic and osteogenic differentiation and the relationship between PD-1 and cell differentiation and SHP2/NF-κB signals.

Methods

SCAPs were obtained culture in the related medium. The proliferation ability was evaluated by cell counting kit 8 and 5-ethynyl-20-deoxyuridine (EdU) assay. Alkaline phosphatase (ALP) activity assay, ALP staining, western blot, real-time RT-PCR, Alizarin Red S staining, and immunofluorescence staining were performed to explore the osteo/odontogenic potential and the involvement of SHP2/NF-κB pathways. Besides, we transplanted SCAPs component into mouse calvaria defects to evaluate osteogenesis *in vivo*.

Results

We found that human SCAPs expressed PD-1 for the first time. PD-1 knockdown enhanced the osteo/odontogenic differentiation of SCAPs by suppressing SHP2 pathway and activating NF-κB pathway. Overexpression of PD-1 inhibited the osteogenesis and odontogenesis of SCAPs via activation of SHP2 signal and inhibition of NF-κB pathway.

Conclusion

PD-1 activated SHP2 signal to block NF-κB signal and then played a vital role in osteo/odontogenic differentiation of SCAPs.

Highlights

1. We found that human SCAPs expressed PD-1 for the first time.
2. PD-1 was found to suppress the osteogenic and odontogenic differentiation of SCAPs *in vitro and in vivo*.
3. SHP2/NF-κB axis was involved in PD-1-mediated SCAPs
4. This study will provide a strong foundation for follow-up clinical trials.

Introduction

Pulp necrosis leads to teeth fracture and a higher incidence of extraction, especially immature tooth[1]. Tooth loss and orofacial bone defects caused by tooth loss have great impact on the patient's chewing efficiency and even the patient's physical health[2]. How to effectively regenerate dentin, promote bone

regeneration and repair hard tissue defects is the key problem in dental regenerative medicine[3,4]. Mesenchymal stem cells (MSCs)-based therapy gradually becomes a promising alternative treatment for regenerative medicine[5]. SCAPs are one type of MSCs residing in the root apex of young permanent teeth, contributing to root dentin formation and root elongation during root maturation[6]. Common to other dental stem cells, SCAPs expressed many MSCs surface markers such as CD29, CD90, CD105, CD73, STRO-1 and negative to hematopoietic cell lineage marker CD45, CD34[7,8]. SCAPs exhibit self-renewal ability and multipotent differentiation[9,10]. The multi-differentiation potential of SCAPs is similar to that of human dental pulp stem cells (hDPSCs). However, SCAPs showed higher proliferation rate and increasingly stronger osteo/odontogenic potential than hDPSCs and human periodontal ligament stem cells (hPDLSCs)[11]. Furthermore, compares with hDPSCs, SCAPs have a higher antiapoptotic survival protein expression, longer telomere length and higher telomerase activity related to cellular lifespan[12,13]. Some studies suggested that residual SCAPs in the apical papilla surviving the infection may induce or at least be partially responsible for the mineralized tissue formation or repair shown in regenerative endodontic treatment[14]. Osteogenic preconditioning prior to transplantation was shown to enhance bone formation at the recipient sites[15,16]. Moreover, SCAPs can be used to reconstruct the spinal cord injury in animal model[17]. When transplanted into immunocompromised mice, SCAPs can form a typical dentin-pulp-like complex and generate bone-like tissues containing osteoblast-like cells[18]. In the case of immature permanent apical lesions, SCAPs can guide the development of root, eventually form the root and promote the healing of periapical tissues. Therefore, SCAPs were considered as a promising alterative seed cell for dentistry regeneration.

PD-1, also referred to as CD279, was first discovered in 1992 as an apoptosis-associated gene[19]. PD-1 is a member of B7/CD28 family and has the similar amino acid sequence of CD28[20,21]. PD-1 is expressed on the surface of various cell types, such as macrophages, dendritic cells, monocytes, activated T cells, B cells and natural killer cells[22,23]. Therefore, PD-1 is extensively studied inhibitory immune checkpoint molecule that mediates the immune escape of tumor cells[24,25]. Among these checkpoints, PD-1 can regulate the proliferation of T cells, cytotoxic secretion in cancer to degenerating anti-tumor immune responses with its ligands[26]. These immune cells may express PD-1 and display higher levels of PD-1. There are two PD-1 ligands in the B7 family: the broadly expressed PD-1 ligand 1 (PD-L1, B7-H1/CD274) and the higher affinity, more restrictedly expressed PD-1 ligand 2 (PD-L2, CD273)[27]. PD-L1 is the immune checkpoint molecule, which is often expressed by a wide variety of cells including both hematopoietic and nonhematopoietic cells[28,29]. PD-L2 expression is more restricted to antigen presenting cells, such as B cells, dendritic cells and macrophages[30]. Under physiological conditions, PD-1 engagement by PD-L1 and PD-L2 regulates over-reactions of immune cells and contribute to maintain peripheral tolerance[31]. However, when PD-L1/PD-L2 are expressed on the surface of tumor cells, T cell-mediated anti-tumor activity may be severely compromised[32]. It was thoughted that PD-1functions exclusively within immune system. Surprisingly, PD-1 was detected in different proportions also in retina ganglion cells and the expression of PD-1 was dramatically found to be upregulated in large retina ganglion cells after optic nerve injury[33]. This is the first report of the expression of PD-1 outside the immune system, and suggests that PD-1 play a new role in maintaining

neuronal function. And new research revealed that DPSCs which derived from neural crest also expressed PD-1[34]. Furthermore, the result showed that PD-1 plays a vital role in maintenance of cell proliferation ability and multipotential differentiation potential of DPSCs. However, it is unknown whether SCAPs also derived from neural crest express PD-1 and whether PD-1 regulates SCAPs function.

Materials And Methods

2.1 Isolation and culture of SCAPs

Teeth were acquired with consent from patients. The apical papilla was separated from root tips, minced and digested with collagenase type I and dispase (Gibco, USA). After digestion, cells were seeded in culture flasks which contained alpha-minimal essential medium (α-MEM; Gibco) with 10% weight per volume (w/v) fetal bovine serum (FBS; BI, Israel) and 1% penicillin-streptomycin (Gibco).

2.2 Characterizations of SCAPs

2.2.1 Immunofluorescence staining

Immunocytochemistry for MSCs marker STRO-1 was used to confirm the cell phenotype. SCAPs were cultured on glass coverslips for 3 days. Cells were washed twice with phosphate buffer saline (PBS; Gibco), fixed in 4% polyoxymethylene (Biosharp, China), permeabilized with 0.5% Triton X-100 (Beyotime, China) and then blocked with bovine serum albumin (BSA, Boster, China). After that, cells were incubated with primary antibody (STRO-1; Santa Cruz) overnight. Cells were incubated in the fluorescence-labeled secondary antibody. 4,6-diamidino-2-phenylindole (DAPI; Beyotime) was used to dye nuclei. Immunofluorescence images were acquired with the microscope (Olympus, Germany).

2.2.2 Colony forming assay

SCAPs were seeded into 6-well plates (Nest, China). 10 days later, SCAPs were fixed, stained with crystal violet (Beyotime). Images were scanned and visualized under the microscope.

2.2.3 Flow cytometric analysis

The characteristic cell surface markers for MSCs were measured by flow cytometric analysis. SCAPs were incubated with fluorochrome-conjugated rabbit anti-human antibodies: CD105, CD90, CD73, CD45, CD34 (BD Biosciences, USA) in the dark atmosphere according to MSCs characterization guidelines[35]. Cells were washed and analyzed by BD FACS (BD Biosciences).

2.2.4 Multipotent differentiation of SCAPs

2.2.4.1 Osteoblastic differentiation induction

Mineralized nodules formation was determined by using alizarin red S (ARS; Sigma, USA) staining. SCAPs were exposed to mineralization induction medium (MM) containing complete medium, 100 nM

dexamethasone (Sigma), 10 mM β-glycerol phosphate (Sigma) and 50 μg/mL ascorbic acid (Sigma) for 14 d. Cells were stained in ARS solution and detected under the microscope.

2.2.4.2 Adipogenic differentiation induction

For lipogenic differentiation, SCAPs were grown in adipogenic induction medium (Cyagen Biosciences, China). Following 4 weeks of induction, lipid droplets were stained with Oil Red O working solution (Cyagen Biosciences) and detected by the microscope.

2.2.4.3 Chondrogenic differentiation induction

For chondrogenic differentiation, SCAPs were exposed to chondrogenic induction medium (Cyagen Biosciences). After 28 days, cells were stained with Alcian Blue (Cyagen Biosciences) and visualized under the microscope.

2.3 Transfection of siRNA

For siRNA transfection, SCAPs were treated with PD-1 siRNA or control vehicle siRNA with CP Regent (Ribo Biotechnology, China). For chemical reagent treatments, SCAPs were treated with 10 μM NF-κB inhibitor (BMS345441; Selleck Chemical), or 50 μM SHP2 inhibitor (NSC87877; Cayman, USA). Treated cells were used for further experiments.

2.4 Lentivirus infection

Lentivirus vectors were bought from Genechem (Shanghai, China). The lentivirus vectors contain a target gene or empty lentiviral vectors. SCAPs were transfected with lentivirus according to the protocol. After 12-16 h, culture medium was replaced with fresh medium.

2.5 Cell counting kit-8 (CCK-8)

The proliferative ability of SCAPs was analyzed by CCK-8 (Dojindo, Japan) assays. Briefly, SCAPs were seeded in 96-well plates. At 0, 1, 3, 5, 7 days, medium was replaced by 10% CCK-8 solution. Samples were incubated for 2 h at 37 °C. The absorbance of each sample was analyzed at 450 nm using a microtiter plate reader (BioTek, UK).

2.6 5–ethynyl-20-deoxyuridine (EdU) assay

SCAPs were seeded on glass coverslips. Cell proliferation ratio was measured using EdU Cell Proliferation Assay Kit (Ribo Biotechnology, China). After exposed to EdU solution, cells were fixed and then permeabilized. After that, SCAPs were reacted with 1×Apollo® reaction cocktail. DNA contents were stained with Hoechst 33342 and visualized under a fluorescent microscope.

2.7 Alkaline phosphatase (ALP) staining and activity assay

After osteoblastic induction for 7 days, SCAPs were rinsed with PBS and fixed. Subsequently, ALP staining was performed using BCIP/NBT ALP Kit (Beyotime). A commercialized ALP activity kit (Nanjing Jiancheng Biology, China) was used to analyze ALP activity. ALP activity was normalized to the total protein content according to relevant formula.

2.8 Calcium Deposition Assay

After osteoblastic induction for 14 d, SCAPs were fixed and stained with ARS solution. Representative images were obtained via microscope. For calcium deposition quantification, calcific deposits were dissolved with 10% cetylpyridinium chloride monohydrate (CPC; Beyotime, China). The absorbance was measured at 562 nm.

2.9 RNA extraction and quantitative reverse-transcription polymerase chain reaction (qRT-PCR)

Total RNA was isolated using TRIzol reagent (Invitrogen Life Technologies, USA) and reverse-transcribed into cDNA with a Reverse Transcription Kit (Vazyme, China). QRT-PCR was performed by SYBR Green Real-Time PCR Master Mix (Vazyme). Cycling conditions as: 95 °C for 30 s and 45 cycles of denaturation at 95°C for 10 s and amplification at 60°C for 30 s. The detailed murine primer sequences of all genes are shown in Table 1. Glyceraldehyde-3-phosphate dehydrogenase (GAPDH) was used as an internal control. The sequences of primers were listed in table 1.

2.10 Western blot analysis

SCAPs were harvested and lysed in radio immunoprecipitation assay (RIPA; Beyotime) lysis buffer containing phosphatase inhibitor and protease inhibitor (Beyotime). Western blot was performed and then transferred to polyvinylidene difluoride membranes (PVDF; Millipore, USA). After blocking with 5% BSA, membranes were probed with primary antibodies against GAPDH (Proteintech. China), DSPP (Bioworld, China), OSX, ALP (Abcam, China), RUNX2, Histone 3 (H3), IκBα, P65, phosphorylated-IκBα (p-IκBα), phosphorylated-P65 (p-P65; Cell Signaling Technology, USA). Next, membranes were incubated with secondary antibodies. Immunoreactive bands on membranes were visualized with an ECL according to instructions provided by the manufacturer.

2.11 Immunofluorescence staining

SCAPs were fixed, permeabilized and blocked. Cells were incubated with primary antibodies against primary antibodies DSPP, RUNX2, P65 as described above. Followed by incubation with specific second antibodies (Abclonal, China), cells were incubated with DAPI. Images were captured by the microscope.

2.12 Animal experiments

All animal experiments were approved by the Institutional Animal Care and Use Committee of Nanjing Medical University (IACUC-2108030). For this study, 6-week-old male Sprague–Dawley (SD) rats were anesthetized with pentobarbital. Two defects with a diameter of 5 mm were drilled on each side of the

cranium using low-speed dental engine with a ring burr. Atelocollagen sponges were used as the scaffold, and were soaked with SCAPs. Scaffolds containing SCAPs were implanted into the defects Finally, the incisions were closed with 4−0 nylon sutures. At 12 weeks after surgery, the rats were sacrificed. The calvarias were used for micro-CT assay and hematoxylin-eosin (H&E) staining.

2.13 micro-CT scanning

To evaluate the bone formation *in vivo*, cranium samples were scanned using a micro-computed tomography (micro-CT) system. After 3D reconstruction, relative bone growth surface area was calculated.

2.14 hematoxylin-eosin (H&E) staining

After micro-CT scanning, calvarias from rats were fixed in 10% neutral formalin for 48 h and then decalcified in ethylenediamine tetra acetic acid (EDTA) for >8 weeks with a solution change every 3 days. Specimens were embedded in paraffin. 5 μm paraffin sections were stained with hematoxylin-eosin (H&E) to visualize any histological changes.

2.15 Statistical analysis

Results were presented as means± standard error of mean. Data for comparisons were analyzed by two-way analysis of variance (ANOVA) for comparisons. *p<0.05* was considered as statistically significant difference.

Table 1. Primer sequences for qRT-PCR analysis of gene expression.

Target gene	Sequences (5¢-3¢)	Product size (bp)
RUNX2	Forward, TCTTAGAACAAATTCTGCCCTTT	136
	Reverse, TGCTTTGGTCTTGAAATCACA	
OSX	Forward, CCTCCTCAGCTCACCTTCTC	148
	Reverse, GTTGGGAGCCCAAATAGAAA	
ALP	Forward, GACCTCCTCGGAAGACACTC	137
	Reverse, TGAAGGGCTTCTTGTCTGTG	
DSPP	Forward, ATATTGAGGGCTGGAATGGGGA	136
	Reverse, TTTGTGGCTCCAGCATTGTCA	
GAPDH	Forward, GAAGGTGAAGGTCGGAGTC	
	Reverse, GAGATGGTGATGGGATTTC	225

Results

3.1 SCAPs isolation, culture and identification

The primary SCAPs were isolated from dental apical papilla. Under the microscope, SCAPs were displayed long spindle shape (Figure 1A). Immunofluorescence staining of cultured SCAPs was counterstained with STRO-1 (red) and DAPI (blue) to visualize cells. The result showed that SCAPs could express MSCs marker STRO-1 (Figure 1B). Flow cytometric results indicated that SCAPs could express MSCs associated markers including CD73, CD105, CD90; but were negative for hematopoietic cell marker CD34 and leucocyte maker CD45 (Figure 1C). Colony formation assay showed that SCAPs formed colonies and a colony was exhibited under the microscope (Figure 1D). After cells cultured in chondrogenic induction medium, chondrogenic differentiation potential of SCAPs was evidenced by Alcian Blue staining (Figure 1E). After osteogenic induction, mineralized calcium deposition was observed in SCAPs (Figure 1F). After adipogenic induction, SCAPs formed a few of fat drops. (Figure 1G).

3.2 PD-1 was downregulated during osteoblastic differentiation of SCAPs

Firstly, immunofluorescence staining showed that PD-1 was expressed in SCAPs (Figure 2A). To explore the role of PD-1 in differentiation of SCAPs, the expression level of PD-1 was determined in SCAPs after cultured in MM for 0, 3 and 7 days. The result of qRT-PCR demonstrated that PD-1 expression was progressively decreased during differentiation of SCAPs (Figure 2B). In addition, western blot results also revealed that PD-1 expression at protein level was gradually downregulated in a time-dependent manner during differentiation of SCAPs (Figure 2C, D). These results confirmed that PD-1 may be associated with differentiation of SCAPs.

3.3 PD-1 did not affect the proliferation of SCAPs

To ascertain the effect of PD-1 on proliferation and differentiation of SCAPs, we used RNA interference technique for suppressing PD-1 levels in SCAPs and lentivirus infection technique for overexpressing PD-1 levels. As is shown in Figure 3A, the mRNA expression level of PD-1 was decreased in small interfering RNAs targeting PD-1 (siPD-1) group compared to the small interfering RNA negative control (NC) group. And the protein expression of PD-1 was lower in siPD-1 group than NC group (Figure 3B, C). Moreover, the mRNA expression level of PD-1 was markedly higher than NC-over group in PD-1-over group (Figure 3D). Western blot analysis revealed the protein expression level of PD-1 was increased in PD-1-over group compared with NC-over group (Figure 3E, F). Immunofluorescence staining showed that PD-1 was downregulated after the transfection of siPD-1 (Figure 3G). Immunofluorescence staining showed that PD-1 was upregulated after the transfection of PD-1 over lentivirus (Figure 3H). The result of CCK-8 showed that PD-1 depletion had no effects on the proliferation of SCAPs (Figure 3I). EdU assay showed no statistical difference in the proliferation of SCAPs between NC group and siPD-1group (Figure 3J, K). CCK-8 assay revealed that PD-1-over did not affect cell growth (Figure 3L). The result of EdU assay confirmed that PD-1-over had no influence on the proliferation potential of SCAPs (Figure 3M, N).

3.4 Knockdown of PD-1 enhanced osteogenic and odontogenic differentiation of SCAPs

In order to elucidate the role of downregulated PD-1 in osteo/ odontogenic differentiation, we inhibited PD-1 expression by using siRNA transfection respectively. ALP activity was higher in the group of siPD-1-transfected cells than NC group by ALP staining and ALP activity assay (Figure 4A, B). Furthermore, mineralization formation of SCAPs was gauged by ARS staining after induction. ARS staining indicated increased calcium deposits formation in SCAPs with siPD-1 transfection (Figure 4C). Moreover, cells in siPD-1 group showed increased mineralization as determined by quantitative calcium measurements (Figure 4D). Meanwhile, qRT-PCR results revealed that the osteo/odontogenic-related genes *DSPP, RUNX2, ALP* and *OSX* were obviously upregulated in the PD-1 knockdown group (Figure 4E). Western blot analysis indicated that the protein expression levels of DSPP, RUNX2, ALP and OSX were induced by PD-1 knockdown (Figure 4F, G). Immunofluorescence staining revealed that PD-1 silence enhanced the expression levels of DSPP, ALP, RUNX2 (Figure 4H, I, J). All these data implied that PD-1 knockdown led to accelerated differentiation of SCAPs.

3.5 Overexpression of PD-1 decreased the osteogenic and odontogenic differentiation of SCAPs

To further determine whether PD-1 was involved in the regulation of osteoblasts and odontoblasts differentiation in SCAPs, lentivirus transfection was conducted to overexpress PD-1. ALP staining and activity assay indicated that ALP activity was decreased in the PD-1 overexpression group (Figure 5A, B). ARS staining and CPC assay showed the decrease of calcium nodules formation in PD-1-over group (Figure 5C, D). The results of qRT-PCR demonstrated that PD-1 upregulation led to a dramatic drop of DSPP, RUNX2, ALP and OSX mRNA (Figure 5E). The regulation of PD-1 overexpression on DSPP, RUNX2, ALP and OSX was further confirmed at protein level (Figure 5F, G). Immunofluorescence staining confirmed that transfection with PD-1 lentivirus decreased the expression of DSPP, ALP and RUNX2 (Figure 5H, I, J). These results above revealed that forced expression of PD-1 could suppress osteogenic and odontogenic differentiation of SCAPs.

3.6 PD-1 inhibited bone healing in a rat calvarial bone defects model

To further evaluate the effect of PD-1 *in vivo*, SCAPs with PD-1 lentivirus transfection or siRNA transfection were used in a rat calvarial bone defects model (Figure 6A). The effect was confirmed by radiographic and histological analysis. The results of microcomputed tomographic (micro-CT) analyses showed significant increase in relative bone growth surface area in siPD-1 group when compared with the NC group (Figure 6B, C). While the area of a newly formed bone in PD-1-over group was lower than that in NC-over group (Figure 6D, E). At 12 weeks, more new bone was formed in bone defects in siPD-1 compared with NC group (Figure 6F). Conversely, little new bone was observed in the PD-1-over group which is much less than that in the NC-over group.

3.7 Knockdown of PD-1 suppressed the phosphorylation of SHP2, overexpression of PD-1 promoted the phosphorylation of SHP2

Western blot showed that the phosphorylation of SHP2 were downregulated in PD-1 knockdown group and NSC87877 inhibition exerted a down-regulation effect on the protein expression of p-SHP2 (Figure

7A, C). PD-1 overexpression upregulated the protein expression of p-SHP2, while the expression of SHP2 had no significant change in trend in PD-1-over group. The protein level of p-SHP2 was down-regulated by inhibitor of SHP2 signal NSC87877 (Figure 7B, D). Further research also showed that NSC87877 enhanced the phosphorylation of IκBα and P65, and promoted the translocation of P65 from cytoplasm to nucleus in PD-1 knockdown group (Figure 7E, G) and PD-1 overexpression group (Figure 7F, H). This result was confirmed by immunofluorescence staining (Figure 7I, J). The results above implied that SHP2 signal blockade played a critical role on the expression of downstream signaling NF-κB pathway in SCAPs.

3.8 Knockdown of PD-1 promoted the translocation of P65 from cytoplasm to nucleus, overexpression of PD-1 suppressed the translocation of P65 from cytoplasm to nucleus

Western blot showed that PD-1 inhibition significantly promoted the phosphorylation of IκBα and P65, and while these effects were weakened by BMS345441 treatment. Knockdown of PD-1 promoted the translocation of P65 from cytoplasm to nucleus, while these effects were weakened by BMS345441 treatment (Figure 8A, C). PD-1 overexpression significantly suppressed the phosphorylation of IκBα and P65, while these effects were furtherly weakened by BMS345441 treatment. PD-1 overexpression inhibited the translocation of P65 from cytoplasm to nucleus, and these effects were weakened by BMS345441 treatment (Figure 8B, D). Immunofluorescence staining revealed that the nuclear P65 expression apparently increased in siPD-1 group, and BMS345441 reduced the nuclear P65 expression (Figure 8E). Immunofluorescence staining revealed that PD-1 overexpression suppressed the nuclear P65 expression, BMS345441 further inhibited the nuclear P65 expression (Figure 8F).

3.9 PD-1 enhanced SCAPs osteogenic and odontogenic differentiation by suppressing SHP2 signal

ALP activity assay and ALP staining showed that in PD-1 blockade group, ALP activity was markedly increased by NSC87877 (Figure 9A, B). Analogously, the downregulation of ALP activity in SCAPs was induced by PD-1 overexpression, and ALP activity of SCAPs could be significantly enhanced by SHP2 inhibitor NSC87877 (Figure 9C, D). Remarkably, the mRNA expression levels of DSPP, RUNX2, ALP and OSX were significantly upregulated in the siPD-1+NSC87877 (Figure 9E). Western blot analysis showed that siPD-1+NSC87877 group expressed markedly increased levels of DSPP, RUNX2, ALP and OSX in comparison with siPD-1 group (Figure 9F, G). Western blot analysis and qRT-PCR were used to measure the expression of osteogenic and odontogenic markers in NC-over, PD-1-over, PD-1-over+NSC87877 groups. QRT-PCR result indicated that the osteogenic and odontogenic differentiation genes in SCAPs were significantly upregulated by NSC87877 (Figure 9H). Western blot analysis indicated that the osteogenic and odontogenic differentiation markers (DSPP, RUNX2, ALP and OSX) in PD-1-over+NSC87877 group were increased compared with PD-1-over group (Figure 9I, J). In addition, we found that knockdown of PD-1 with NSC87877 enhanced the osteogenic and odontogenic differentiation markers (DSPP and RUNX2) by immunofluorescence staining (Figure 9K, L). We observed a significant increase of DSPP and RUNX2 in PD-1-over+ NSC87877 group vs PD-1-over group (Figure 9M, N). Taken

together, these results pointed out that inhibition of SHP2 signal promoted osteogenic and odontogenic differentiation of SCAPs.

3.10 PD-1 inhibited SCAPs osteogenic and odontogenic differentiation by enhancing NF-κB signaling

ALP activity was markedly decreased in siPD-1+BMS345441 groups (Figure 10A, B; $p<0.01$). ALP staining and ALP activity assay showed PD-1-over+BMS345441 resulted in a significantly reduced ALP activity (Figure 10C, D). Consistently, qRT-PCR further confirmed that the downregulation of DSPP, RUNX2, ALP and OSX induced by PD-1 overexpression could be partially blocked by NF-κB signal inhibitor BMS345441 (Figure 10E). Western blot shoed that PD-1 knockdown enhanced DSPP, RUNX2, ALP and OSX protein expression, whereas co-transfection with PD-1 siRNA and BMS345441 reversed the repression of DSPP, RUNX2, ALP and OSX protein levels (Figure 10F, G). QRT-PCR showed that the osteogenic and odontogenic markers were also decreased in PD-1-over+BMS345441 group (Figure10H). The decreased levels of DSPP, RUNX2, ALP and OSX protein were found in the PD-1-over+BMS345441 group in comparison to PD-1-over group (Figure 10I, J). Immunofluorescence staining revealed that siPD-1+BMS345441 group had a reduced expression level of DSPP and RUNX2 in comparison to siPD-1 group (Figure 10K, L). Immunofluorescence staining showed that decreased expressions of osteo/odontogenesis-related markers DSPP and RUNX2 were observed in PD-1-over+BMS345441 group (Figure 10M, N). The data revealed that inhibition of NF-κB signal could suppress osteogenesis and odontogenesis of SCAPs.

Discussion

Stem cell-based therapy has attracted great interest for the treatment of multiple diseases[36]. MSCs derived from dental tissues are perceived as a promising source of cells with therapeutic potential, especially for dental tissue treatment. Orofacial tissue regeneration and repair of tissues depend on MSCs[37]. Dental apical papilla directly contributes toward tooth development and regeneration[38]. SCAPs located around the open apex of premature tooth root are able to undergo multilineage differentiation and possess low immunogenicity, which could contribute to tissue engineering and regenerative therapy[39]. As such, SCAPs become an easily accessible source of cell-based regenerative therapies. The maintenance of self-renewal and differentiation potential plays a pivotal role in MSCs-based therapy, but expansion *in vitro* may lead to the loss of these characteristics[40]. Therefore, improving the function of MSCs will effectively promote the therapeutic efficacy of MSCs[41]. Our research revealed that SCAPs can express PD-1. Moreover, knockdown of PD-1 enhanced osteo/odontogenic differentiation of SCAPs, and overexpression of PD-1 repressed osteogenic and odontogenic differentiation of SCAPs.

PD-1 belongs to the immunoglobulin superfamily[42]. The expression of PD-1 in T and B cells is inducible upon stimulation[43]. PD-1 is not only a potent T cell inhibitor with a critical role in peripheral tolerance, but also a negative costimulatory receptor critical for the suppression of T cell activation *in vitro* and *in vivo*[44,45]. Recently, some studies revealed constitutive expression of PD-1 in neurons of the mouse retina

and brain[46]. Furthermore, PD-1 expression was shown to be significantly increased in retina ganglion cells after a crushing injury to the optic nerve, suggesting that PD-1 might be essential in retinal neurodegeneration[47]. Recently, Oldenhove et al. demonstrated that PD-1 expression on type 2 innate lymphoid cells can result in the dysregulation of tissue metabolism[48]. Furthermore, during *in vitro* cultivation, PD-1 blockade altered the differentiation kinetics[44]. In fact, it had been confirmed that PD-1 knockout can affect the proliferation and differentiation of stem cells[34]. In view of important findings of this study, it is crucial to acquire information on the expression and on physiological aspects of PD-1 in SCAPs. Moreover, PD-1 was lowly expressed during mineralization induction of SCAPs. We demonstrated that PD-1 was increased by five-fold in PD-1 lentivirus transfection overexpression group, and reduced in the PD-1 knockdown group. Previously, several articles have reported the strategy of intrinsic blockade of PD-1 in cells with CRISPR/Cas9 or shRNA technologies[49]. Therefore, PD-1 silencing would accelerate the osteo/odontogenic differentiation of SCAPs and PD-1 overexpression impaired the osteo/odontogenic differentiation of SCAPs. However, the regulatory mechanism of PD-1 in osteo/odontogenic differentiation of SCAPs needs to be explored further.

PD-1 contains two different signaling motifs in its cytoplasmic tail, an immunoreceptor tyrosine-based inhibition motif (ITIM) and an immunoreceptor tyrosine-based switch motif (ITSM)[50]. Phosphorylation of both motifs above recruits the protein tyrosine phosphatases (PTPs), such as Src homology 2 domain−containing tyrosine phosphatase 2 (SHP2)[51]. Increasing evidence has revealed these PTPs can dephosphorylate various key signaling pathway kinases and counter the positive signaling events[51]. Moreover, SHP2 is a key downstream effector of the immune checkpoint receptor PD-1 in T cells[52]. Tyrosine phosphatase SHP2 is an intracellular domain responsible for transmission of inhibitory signals in PD-1/PD-L pathway[50,53]. In this study, we investigated that upregulation of PD-1 enhanced the phosphorylate of SHP2, while downregulation of PD-1 inhibited the phosphorylate of SHP2.

SHP2, a ubiquitously expressed multifunctional protein, is a major phosphatase involved in several cellular processes. PD-1-associated SHP2 dephosphorylates downstream pathway. Eventually, PD-1 signaling transduction leads to decreased activation of transcription factors, such as NF-κB pathway[54]. NF-κB signaling pathway is an important regulator of cellular gene transcription and can regulate differentiation[55]. When cells are induced by inflammatory complement, oxidative stress and other factors, leading to NF-κB pathway activation[56]. The activation of NF-κB pathway is characterized by the phosphorylation of P65 and IκBα in the cytoplasm, the translocation of P65 into the nucleus[57]. Therefore, we investigated the expression of P65 in nucleus to demonstrate whether PD-1 inhibited SCAPs osteoblastic and odontoblastic differentiation by suppressing NF-κB signal. The result of this study demonstrated that knockdown of PD-1 enhanced the osteogenic and odontogenic differentiation via activating NF-κB signaling pathway and overexpression of PD-1 inhibited the osteogenic and odontogenic differentiation via suppressing NF-κB signaling pathway. In this study, we revealed that PD-1 was confirmed to regulate negatively osteogenesis and odontogenesis due to its inhibition resulted in the osteogenesis and odontogenesis enhancement and its overexpression resulted in the osteogenesis and odontogenesis inhibition.

Furthermore, our data illustrated that PD-1 functioned as an inhibitor in osteogenesis and odontogenesis of SCAPs. NF-κB signal functioned negative downstream of SHP2 to promote the differentiation of SCAPs. Here, we discussed the detailed effect of PD-1 in these signaling events and their implications in mediating the mechanisms that inhibit differentiation of SCAPs in response to PD-1-mediated signals.

Conclusion

In summary, our findings indicated that PD-1 *in vitro* expressed in SCAPs and played an inhibitory role in the osteogenesis and odontogenesis of SCAPs. The decrease of PD-1 inhibited SHP2 and then activated NF-κB signaling pathway. The increase of PD-1 activated SHP2 and then inhibited NF-κB pathway. These results help to determine the possible mechanism of PD-1 in regulating SCAPs differentiation. This research provides useful insight into the role of PD-1 in SCAPs and offers a theoretical basis for research on applications of SCAPs in tissue engineering.

Abbreviations

ALP: alkaline phosphatase; ARS: alizarin red staining; α-MEM: alpha-minimal essential medium; BMSCs: bone marrow stem cells; BSA: bovine serum albumin; CCK-8: cell counting kit-8 assays; CPC: cetylpyridinium chloride; DAPI: 4' , 6-diamino-2-phenylindole; DPSCs: dental pulp stem cells; DSPP: dentin sialophosphoprotein; EdU assay: 5-Ethynyl-2⍰-Deoxyuridine assay; FBS: fetal bovine serum; GAPDH: glyceraldehyde-3-phosphate dehydrogenase; ITIM: immunoreceptor-tyrosine-inhibitory motif; ITSM: immunoreceptor-tyrosine-switch motif; microCT: microcomputed tomographic; MM: mineralization induction medium; MSCs: mesenchymal stem cells; OSX: osterix; PD-1: programmed cell death protein 1; PDL-1: programmed cell death 1 ligand 1; PDL-2: programmed cell death 1 ligand 2; PDLSCs: periodontal ligament stem cells; RCT: root canal treatment; RUNX2: runt-related transcription factor 2; SCAPs: stem cells from the apical papilla; SHP2: Src homology-2-containing protein tyrosine phosphatase 2

Declarations

Acknowledgements

Conflict of interest

Authors declare no conflicts of interest.

Authors Contributions

Na Li conceived and designed the study, collected and assembled data, and wrote the manuscript. Zehan Li and Lin Fu performed data analysis and interpretation. Ming Fu, Yanqiu Wang completed data analysis

and interpretation. Jintao Wu reviewed data. Jinhua Yu conceived and designed the study, provided financial support and study material, performed the data analysis and interpretation, and approved the final version of the manuscript. All authors read and approved the manuscript.

Availability of data and materials

Datasets used and analyzed during the current study are available from the corresponding author on reasonable request.

Ethics approval and consent to participate

Studies were carried out in accordance with the Declaration of Helsinki and got the approval of the Ethical Committee of Nanjing Medical University.

Consent for publication

Not applicable.

References

1.	Y-L Ng VM, K Gulabivala. Tooth survival following non-surgical root canal treatment: a systematic review of the literature. International Endodontic Journal. 2010; 43(3): 171-89.

2.	Haoqing Yang YL, Yangyang Cao, Yu Cao, Zhipeng Fan. Homeobox C8 inhibited the osteo-/dentinogenic differentiation and migration ability of stem cells of the apical papilla via activating KDM1A. Journal of Cellular Physiology. 2020; 235(11): 8432-45.

3.	Wen Zhang XZ, Junyuan Li, Jianmao Zheng, Xiaoli Hu, Meng Xu, Xueli Mao, Junqi Ling. Foxc2 and BMP2 Induce Osteogenic/Odontogenic Differentiation and Mineralization of Human Stem Cells from Apical Papilla. stem cells International. 2018; 25(2018): 2363917.

4.	Yao Li MY, Zilu Wang, Yangyu Zheng, Junjun Li, Shu Ma, Genxia Liu and Jinhua Yu. 17beta-estradiol promotes the odonto/osteogenic differentiation of stem cells from apical papilla via mitogen-activated protein kinase pathway. Stem Cell Research & Therapy. 2014; 5(6): 125.

5.	Fereshteh Karamali M-HNE, Sara Taleahmad, Leila Satarian, Hossein Baharvand. Stem cells from apical papilla promote differentiation of human pluripotent stem cells towards retinal cells. Differentiation. 2018; 102: 8-15.

6.   Zeni Liu YL, Xiaolin Fang, Jingwen Yang, Zhi Chen. Epigallocatechin-3-Gallate Promotes Osteo-/Odontogenic Differentiation of Stem Cells from the Apical Papilla through Activating the BMP–Smad Signaling Pathway. Molecules. 2021; 26(6): 1580.

7.   Gianrico Spagnuolo BC, Massimo Marrelli, Carlo Rengo, Sandro Rengo, Marco Tatullo. Commitment of Oral-Derived Stem Cells in Dental and Maxillofacial Applications. Dental Journal (Basel). 2018; 6(4): 72.

8.   Ola A Nada RMEB. Stem Cells From the Apical Papilla (SCAP) as a Tool for Endogenous Tissue Regeneration. Frontiers in Bioengineerings and Biotechnology. 2018; 6: 103.

9.   Yosuke Tanaka SS, Haruyoshi Yamaza, Sara Murata, Kento Nishida, Shion Hama, Yukari Kyumoto-Nakamura, Norihisa Uehara, Kazuaki Nonaka, Toshio Kukita, Takayoshi Yamaza. Suppression of AKT-mTOR signal pathway enhances osteogenic/dentinogenic capacity of stem cells from apical papilla. Stem Cell Reserch Ⓔ Therapy. 2018; 9(1).

10.   Xiao Lin RD, Shu Diao, Guoxia Yu, Liping , Zhipeng Fan. SFRP2 enhanced the adipogenic and neuronal differentiation potentials of stem cells from apical papilla. Cell Biology International. 2017; 41(5): 534-43.

11.   Ke Chen HX, Yibin Huang, Caiqi Liu. Comparative analysis of in vitro periodontal characteristics of stem cells from apical papilla (SCAP) and periodontal ligament stem cells (PDLSCs). Archive Oral Biology. 2013; 58(8): 997-1006.

12.   Haoqing Yang GL, Nannan Han, Xiuli Zhang, Yangyang Cao, Yu Cao, Zhipeng Fan. Secreted frizzled-related protein 2 promotes the osteo/ odontogenic differentiation and paracrine potentials of stem cells from apical papilla under inflammation and hypoxia conditions. Cell Proliferation. 2020; 53(1): e12694.

13.   A Bakopoulou GL, J Volk, A Tsiftsoglou, P Garefis, P Koidis, W Geurtsen. Comparative analysis of in vitro osteo/odontogenic differentiation potential of human dental pulp stem cells (DPSCs) and stem cells from the apical papilla. Archives Oral Biology. 2011; 56(7): 709-21.

14.   Vanessa Chrepa BP, Michael A Henry, Anibal Diogenes. Survival of the Apical Papilla and Its Resident Stem Cells in a Case of Advanced Pulpal Necrosis and Apical Periodontitis. Journal of Endodontics. 2017; 43(4): 561-7.

15.   J N Harvestine TG-F, A Sebastian, N R Hum, D C Genetos, G G Loots, J K Leach. Osteogenic preconditioning in perfusion bioreactors improves vascularization and bone formation by human bone marrow aspirates. Science Advances. 2020; 6(7): eaay2387.

16.   Shuntaro Yamada MAY, Thomas Schwarz, Jan Hansmann, Kamal Mustafa. Induction of osteogenic differentiation of bone marrow stromal cells on 3D polyester-based scaffolds solely by

subphysiological fluidic stimulation in a laminar flow bioreactor. Journal of Tissue and Engineering. 2021; (12): 20417314211019375.

17. De Berdt P VJ, Ucakar B, Elens L, Diogenes A, Leprince JG, Deumens R, des Rieux A. Dental Apical Papilla as Therapy for Spinal Cord Injury. Journal of Dental Research. 2015; 9411(11): 1575-81.

18. Shigehiro Abe SY, Akihiko Watanabe, Keiichi Hamada, Teruo Amagasa. Hard tissue regeneration capacity of apical pulp derived cells (APDCs) from human tooth with immature apex. Biochemical Biophysical Research Communications. 2008; 371(1): 90-3.

19. Y Ishida YA, K Shibahara, T Honjo. Induced expression of PD-1, a novel member of the immunoglobulin gene superfamily, upon programmed cell death. The EMBO Journal. 1992; 11(11): 3887-95.

20. Yonghong Zhang LM, Xiaohui Hu, Jinlu Ji, Gil Mor, Aihua Liao. The role of the PD-1/PD-L1 axis in macrophage differentiation and function during pregnancy. Human Reproduction. 2019; 34(1): 25-36.

21. W Chen JW, L Jia, J Liu, Y Tian. Attenuation of the programmed cell death-1 pathway increases the M1 polarization of macrophages induced by zymosan. Cell Death◌Disease. 2016; 7(2): e2115.

22. Kathlenn Liezbeth Oliveira Silva VMC, Gabriela Luvizotto Venturin, Aline Aparecida Correa Leal, Breno Fernando de Almeida, Flavia De Rezende Eugenio, Paulo Sergio Patto Dos Santos, Gisele Fabrino Machado, Valeria Marçal Felix De Lima◌. PD-1 and PD-L1 regulate cellular immunity in canine visceral leishmaniasis. Comparative Immunology, Microbiology and Infectious Diseases. 2019; 62(2019): 76-87.

23. Alexander P R Bally PL, Yan Tang, James W Austin, Christopher D Scharer, Rafi Ahmed, Jeremy M Boss. NF-κB regulates PD-1 expression in macrophages. Journal of Immunology. 2015; 194(9): 4545-54.

24. Wei Xie LJM, Shaoying Li, C Cameron Yin, Joseph D Khoury, Jie Xu. PD-1/PD-L1 Pathway and Its Blockade in Patients with Classic Hodgkin Lymphoma and Non-Hodgkin Large-Cell Lymphomas. Curr Hematol Malig Rep. 2020; 15(4): 372-81.

25. Xiaodong Wang XY, Chang Zhang, Yang Wang, Tianyou Cheng, Liqiang Duan, Zhou Tong, Shuguang Tan, Hangjie Zhang, Phei Er Saw, Yinmin Gu, Jinhua Wang, Yibi Zhang, Lina Shang, Yajuan Liu, Siyuan Jiang, Bingxue Yan, Rong Li, Yue Yang, Jie Yu, Yunzhao Chen, George Fu Gao, Qinong Ye, Shan Gao. Tumor cell-intrinsic PD-1 receptor is a tumor suppressor and mediates resistance to PD-1 blockade therapy. Proceedings of the National Academy Science of the United States of American. 2020; 117(12): 6640-50.

26. Francesca R Mariotti SP, Tiziano Ingegnere, Nicola Tumino, Francesca Besi, Francesca Scordamaglia, Enrico Munari, Silvia Pesce, Emanuela Marcenaro, Alessandro Moretta, Paola Vacca,

Lorenzo Moretta. PD-1 in human NK cells: evidence of cytoplasmic mRNA and protein expression. Oncoimmunology. 2018; 8(3): 1557030.

27.   Yu Liu SL, Chenhua Wu, Wenjing Huang, Bin Xu, Shuai Lian, Li Wang, Shan Yue, Nannan Chen, Zhanbo Zhu. PD-1-Mediated PI3K/Akt/mTOR, Caspase 9/Caspase 3 and ERK Pathways Are Involved in Regulating the Apoptosis and Proliferation of CD4+ and CD8+ T Cells During BVDV Infection in vitro. Frontiers in Immunology. 2020; 11: 467.

28.   Taku Okazaki TH. PD-1 and PD-1 ligands: from discovery to clinical application. International Immunology. 2007; 19(7): 13-24.

29.   Xiaojuan Wang WKKW, Jing Gao, Zhongwu Li, Bin Dong, Xiaoting Lin, Yilin Li, Yanyan Li, Jifang Gong, Changsong Qi, Zhi Peng, Jun Yu, Lin Shen. Autophagy inhibition enhances PD-L1 expression in gastric cancer. Journal of Experimental Clinical Cancer Research. 2019; 38(1): 140.

30.   Jennifer H Yearley CG, Ni Yu, Christina Moon, Erin Murphy, Jonathan Juco, Jared Lunceford, Jonathan Cheng, Laura Q M Chow, Tanguy Y Seiwert, Masahisa Handa, Joanne E Tomassini, Terrill McClanahan. PD-L2 Expression in Human Tumors: Relevance to Anti-PD-1 Therapy in Cancer. Clinical Cancer Research. 2017; 23(12): 3158-67.

31.   Yinan Dong QS, Xinwei Zhang PD-1 and its ligands are important immune checkpoints in cancer. Oncotarget. 2017; 8(2): 2171-86.

32.   Alessandra Dondero FP, Mariella Della Chiesa, Maria Valeria Corrias, Fabio Morandi, Vito Pistoia, Daniel Olive, Francesca Bellora, Franco Locatelli, Aurora Castellano, Lorenzo Moretta, Alessandro Moretta, Cristina Bottino, Roberta Castriconi. PD-L1 expression in metastatic neuroblastoma as an additional mechanism for limiting immune surveillance. Oncoimmunology. 2015; 5(1): e1064578.

33.   Wei Wang AC, Yu Qin, Jacky M K Kwong, Joseph Caprioli, Ralph Levinson, Ling Chen, Lynn K Gordon. Programmed Cell Death-1 is Expressed in Large Retinal Ganglion Cells And is Upregulated After Optic Nerve Crush. Exp Eye Res. 2015; 140: 1-9.

34.   Yao Liu HJ, Xiaoxing Kou, Chider Chen, Dawei Liu, Yan Jin, Li Lu, Songtao Shi. PD-1 is required to maintain stem cell properties in human dental pulp stem cells. Cell Death & Differentiation. 2018; 25(7): 1350-60.

35.   E M Horwitz KLB, M Dominici, I Mueller, I Slaper-Cortenbach, F C Marini, R J Deans, D S Krause, A Keating. The International Society for Cellular Therapy position statement. Cytotherapy. 2005; 7(5): 393-5.

36.   Qiaoqiao Jin KY, Wenzhen Lin, Chenguang Niu, Rui Ma, Zhengwei Huang. Comparative characterization of mesenchymal stem cells from human dental pulp and adipose tissue for bone regeneration potential. Artificial Cells Nanomedicine Biotechnology. 2019; 47(1): 1577-84.

37.	Andrea Ballini AB, Rajiv Saini, Phuc Van Pham, Marco Tatullo. Dental-derived stem cells and their secretome and interactions with bioscaffolds/biomaterials in regenerative medicine: from the in vitro research to translational applications. Stem Cells International. 2017; 2017: 6975251.

38.	George T-J Huang WS, Yi Liu, He Liu, Songlin Wang, Songtao Shi. The hidden treasure in apical papilla: the potential role in pulp/dentin regeneration and bioroot engineering. Journal of Endodontics. 2008; 34(6): 645-51.

39.	Jun Kang WF, Qianyi Deng, Hongwen He, Fang Huang. Stem Cells from the Apical Papilla: A Promising Source for Stem Cell-Based Therapy. Biomedicine Research International. 2019; 2019: 6104738.

40.	A Ballini ADB, D De Vito, A Scarano, S Scacco, L Perillo, F Posa, G Dipalma, F Paduano, M Contaldo, M Grano, G Brunetti, G Colaianni, M Di Cosola, S Cantore, G Mori. Stemness genes expression in naïve vs. osteodifferentiated human dental-derived stem cells. European Reviews for Medicine Pharmacology Science. 2019; 23(7): 2916-23.

41.	Chen Zhang XH, Yuncun Liang, Huina Liu, Zhipeng Fan, Jianpeng Zhang. The Histone Demethylase KDM3B Promotes Osteo-/Odontogenic Differentiation, Cell Proliferation, and Migration Potential of Stem Cells from the Apical Papilla. Stem Cells International. 2020; 2020: 8881021.

42.	Nikolaos Patsoukis DS, Vassiliki A Boussiotis. PD-1 inhibits T cell proliferation by upregulating p27 and p15 and suppressing Cdc25A. Cell Cycle. 2012; 11(23): 4305-9.

43.	Y Agata AK, H Nishimura, Y Ishida, T Tsubata, H Yagita, T Honjo. Expression of the PD-1 antigen on the surface of stimulated mouse T and B lymphocytes. International Immunology. 1996; 8(5): 765-72.

44.	Jianshu Wei CL, Yao Wang, Yelei Guo, Hanren Dai, Chuan Tong, Dongdong Ti, Zhiqiang Wu, Weidong Han PD-1 silencing impairs the anti-tumor function of chimeric antigen receptor modified T cells by inhibiting proliferation activity. Journal of Immunotherapy Cancer. 2019; 7(1): 209.

45.	Tim Wartewig ZK, Selina Keppler, Konstanze Pechloff, Erik Hameister, Rupert Öllinger, Roman Maresch, Thorsten Buch, Katja Steiger, Christof Winter, Roland Rad, Jürgen Ruland. PD-1 is a haploinsufficient suppressor of T cell lymphomagenesis. Nature. 2017; 552(7683): 121-5.

46.	Ling Chen VP, Ralph Levinson, Arlene H Sharpe, Gordon J Freeman, Jonathan Braun, Lynn K Gordon. Constitutive Neuronal Expression of the Immune Regulator, Programmed Death 1 (PD-1), Identified During Experimental Autoimmune Uveitis. Ocular Immunology and Inflammation. 2009; 17(1): 45-55.

47.	Wei Wang AC, Yu Qin, Jacky M. K. Kwong, Joseph Caprioli, Ralph Levinson, Ling Chen, and Lynn K Gordon. Programmed Cell Death-1 is Expressed in Large Retinal Ganglion Cells And is Upregulated After Optic Nerve Crush. Experimental Eye Research. 2015; 140: 1-9.

48.   Guillaume Oldenhove EB, Anaelle Taquin, Valérie Acolty, Lynn Bonetti, Bernhard Ryffel, Marc Le Bert, Kevin Englebert, Louis Boon, Muriel Moser. PD-1 is involved in the dysregulation of type 2 innate lymphoid cells in a murine model of obesity. Cell Reports. 2018; 25(8): 2053-60.

49.   Yasuo Ouchi AP, Yusuke Tamura, Hiroshi Nishimasu, Aina Negishi, Sudip Kumar Paul, Naoki Takemura, Takeshi Satoh, Yasumasa Kimura, Makoto Kurachi, Osamu Nureki, Kenta Nakai, Hiroshi Kiyono, Satoshi Uematsu. Generation of tumor antigen-specific murine CD8+ T cells with enhanced anti-tumor activity via highly efficient CRISPR/Cas9 genome editing. International Immunology. 2018; 30(4): 141-54.

50.   H Nishimura TO, Y Tanaka, K Nakatani, M Hara, A Matsumori, S Sasayama, A Mizoguchi, H Hiai, N Minato, T Honjo. Autoimmune dilated cardiomyopathy in PD-1 receptor-deficient mice. Science. 2001; 291(5502): 319-22.

51.   Tadashi Yokosuka MT, Wakana Kobayashi-Imanishi, Akiko Hashimoto-Tane, Miyuki Azuma, Takashi Saito. Programmed cell death 1 forms negative costimulatory microclusters that directly inhibit T cell receptor signaling by recruiting phosphatase SHP2. The Journal of Experimental Medicine. 2012; 209(6): 1201-17.

52.   M. Marasco AB, J. Weyershaeuser, N. Thorausch, J. Sikorska, J. Krausze, H. J. Brandt, J. Kirkpatrick, P. Rios, W. W. Schamel, M. Köhn, and T. Carlomagno. Molecular mechanism of SHP2 activation by PD-1 stimulation. Science Advances. 2020; 6(5): eaay4458.

53.   Zhenzhen Fan YT, Zhipeng Chen, Lu Liu, Qian Zhou, Jingjing He, James Coleman, Changjiang Dong, Nan Li, Junqi Huang, Chenqi Xu, Zhimin Zhang, Song Gao, Penghui Zhou, Ke Ding and Liang Chen. Blocking interaction between SHP2 and PD-1 denotes a novel opportunity for developing PD-1 inhibitors. EMBO Molecular Medicine. 2020; 12(8): e11571.

54.   Xiaomo Wu ZG, Yang Chen, Borui Chen, Wei Chen, Liqiang Weng, Xiaolong Liu. Application of PD-1 Blockade in Cancer Immunotherapy. Computational and Structural Biotechnology Journal. 2019; 17: 661-74.

55.   Yanqiu Wang YZ, Lin Jin, Xiyao Pang, Yadie Lu, Zilu Wang, Yan Yu, Jinhua Yu. Mineral trioxide aggregate enhances the osteogenic capacity of periodontal ligament stem cells via NF-κB and MAPK signaling pathways. Journal of Cellular Physiology. 2018; 233(3

): 2386-97.

56.   Na Li ZL, Yanqiu Wang, Yan Chen, Xingyun Ge, Jiamin Lu, Minxia Bian, Jintao Wu, Jinhua Yu. CTP-CM enhances osteogenic differentiation of hPDLSCs via NF-κB pathway. Oral Diseases. 2021; 27(3): 577-88.

57. He Liang XY, Chao Liu, Zhongyi Sun, Xiaobin Wang. Effect of NF-kB signaling pathway on the expression of MIF, TNF-α, IL-6 in the regulation of intervertebral disc degeneration. Journal of Musculoskeletal Neuronal Interactions. 2018; 18(4): 551-6.
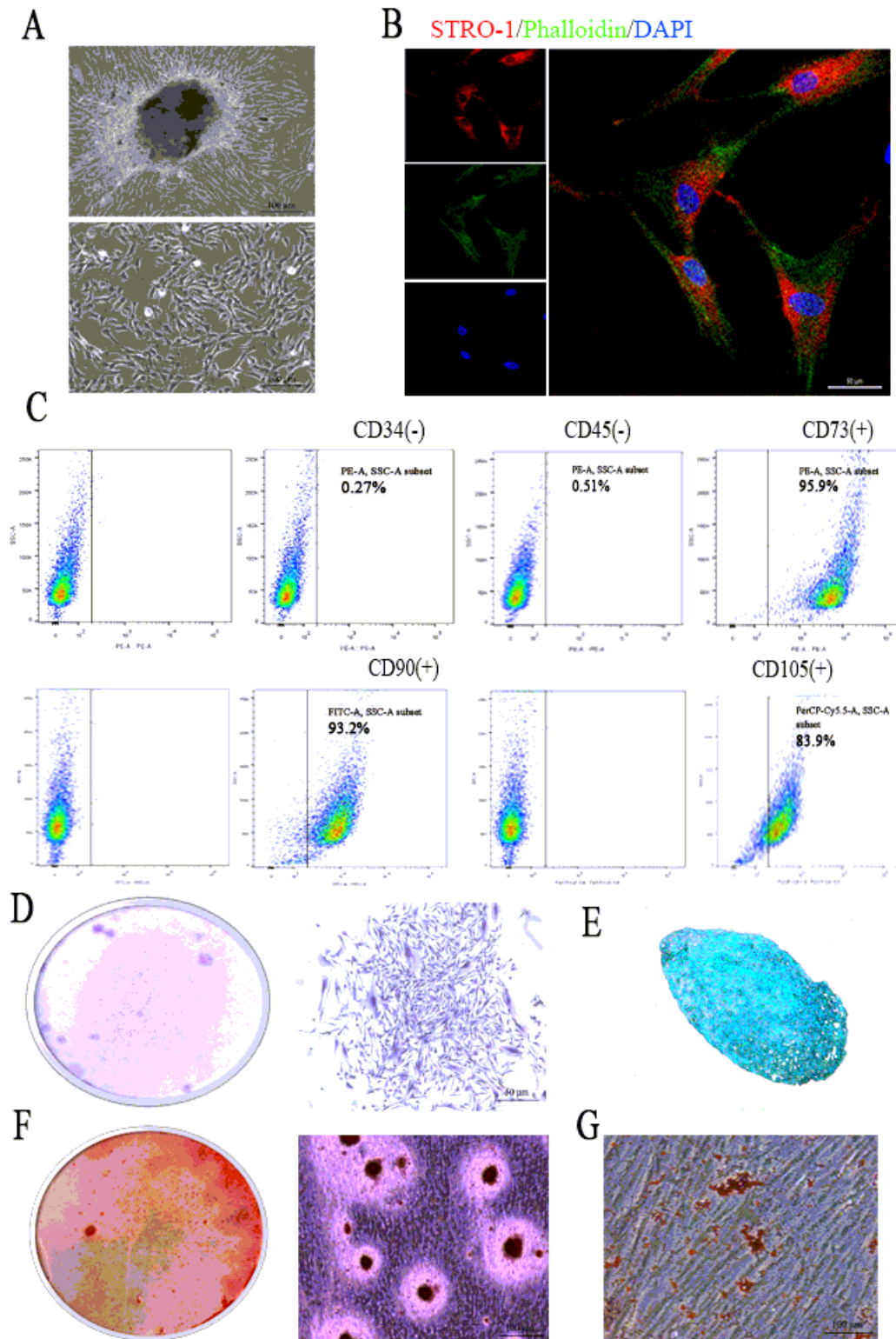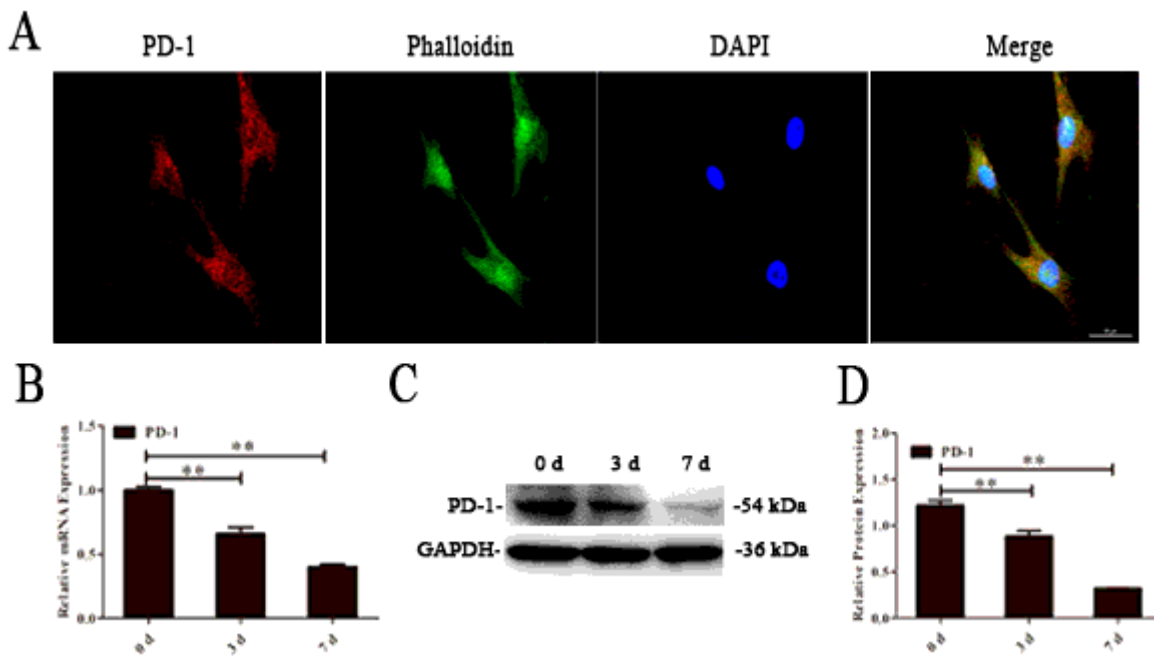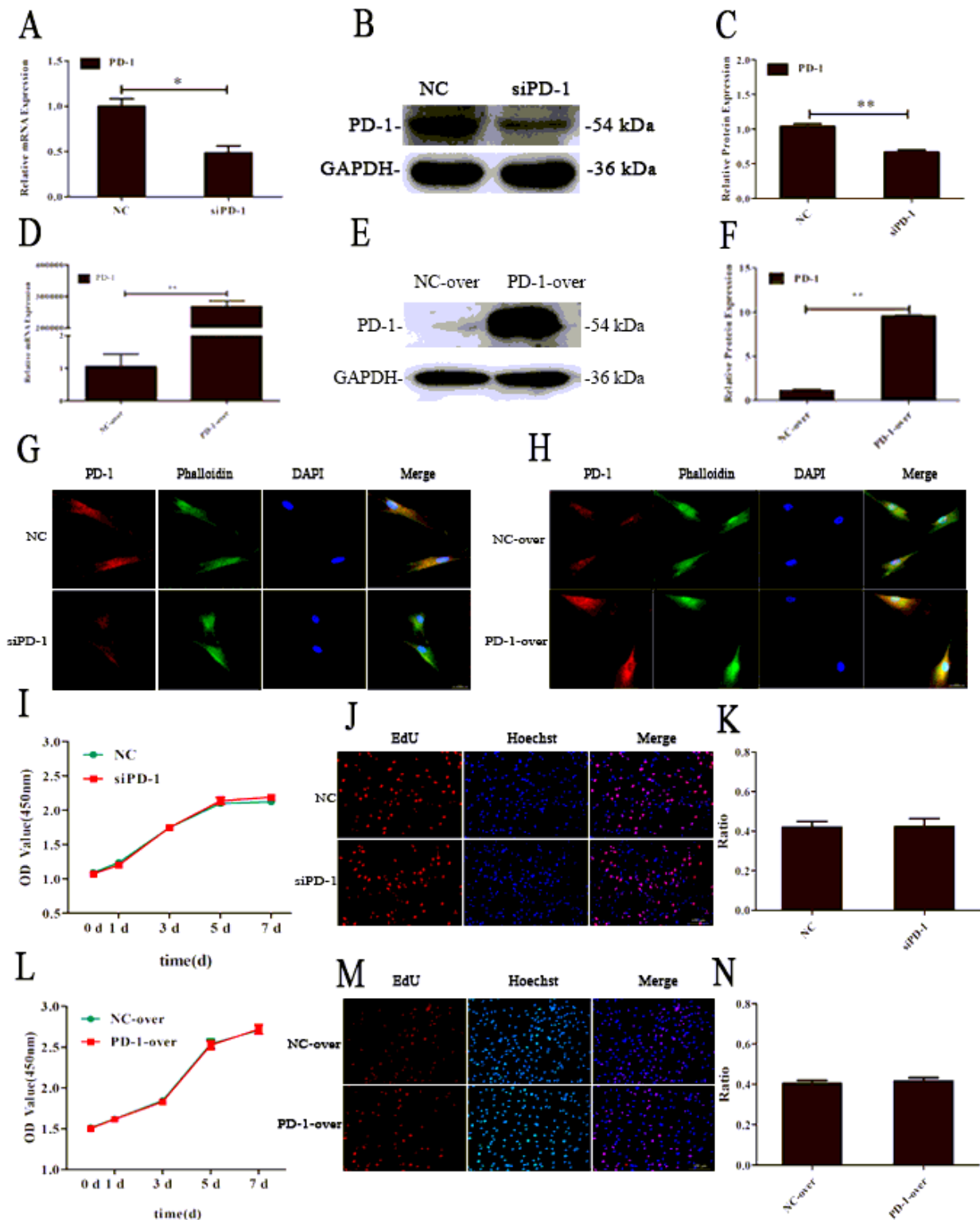
Figures

Figure 1

Characterization of SCAPs (A) SCAPs grown in culture medium. Primary culture (above) and culture at passage 3 (below) were shown (scale bar=100 μm); (B) Immunofluorescence analysis of cultured SCAPs for STRO-1 (red), and nuclei were stained with DAPI (blue) (scale bar=50 μm); (C) Phenotype analysis of SCAPs was conducted by flow cytometric assay. Cell surface markers: CD34 (0.27%), CD45 (0.51%), CD73 (95.9%), CD90 (93.2%), CD105 (83.5%); (D) Single colonies were stained with toluidine blue; (E) Chondrogenic differentiation of SCAPs was determined with Alcian Blue; (F) Osteogenic differentiation of SCAPs was found by ARS staining (scale bar=100 μm); (G) Adipogenic differentiation of SCAPs was determined by Oil red O staining (scale bar=100 μm).

Figure 2

PD-1 was down-regulated during the osteogenic differentiation of SCAPs (A) Immunofluorescence staining showed that PD-1 expressed in SCAPs (scale bar=50 μm); (B) Relative expression of PD-1 was determined by qRT-PCR analysis (*p<0.05, **p<0.01); (C) Western blot analysis of PD-1 at indicated time points; (D) Quantitation of protein band of PD-1 in (C) (*p<0.05, **p<0.01).

Figure 3

PD-1 knockdown and PD-1 overexpression showed no significant effect on the proliferation of SCAPs (A)
The mRNA expression of PD-1 in SCAPs after transient transfection by siRNA (*p<0.05, **p<0.01); (B) The
protein expression of PD-1 was examined by western blot analysis; (C) Quantitation of protein band of
PD-1 in (B) (*p<0.05, **p<0.01); (D) The gene expression of PD-1 was detected by qRT-PCR after
transfection of PD-1-over (*p<0.05, **p<0.01); (E) Western blot analysis of the PD-1 expression in SCAPs;

(F) Quantitation of protein bands of PD-1 in (B) (*p<0.05, **p<0.01); (G) Immunofluorescence staining indicated that PD-1 expressions were lower in siPD-1 group than control group (scale bar=50 μm); (H) Immunofluorescence staining indicated that PD-1 expression was higher in PD-1-over group than control group (scale bar=50 μm); (I) CCK-8 result showed that there is no significant difference between PD-1 knockdown and control group (p>0.05); (J) EdU staining showed that PD-1 knockdown has no effect on the proliferation of SCAPs (scale bar=100 μm); (K) Relative quantitative analysis of EdU staining (p>0.05); (L) CCK-8 result showed that there is no significant difference between PD-1-over group and NC-over group (p>0.05); (M) EdU staining showed that PD-1 overexpression has no effect on the proliferation of SCAPs (scale bar=50 μm); (N) Relative quantitative analysis of EdU staining (p>0.05).
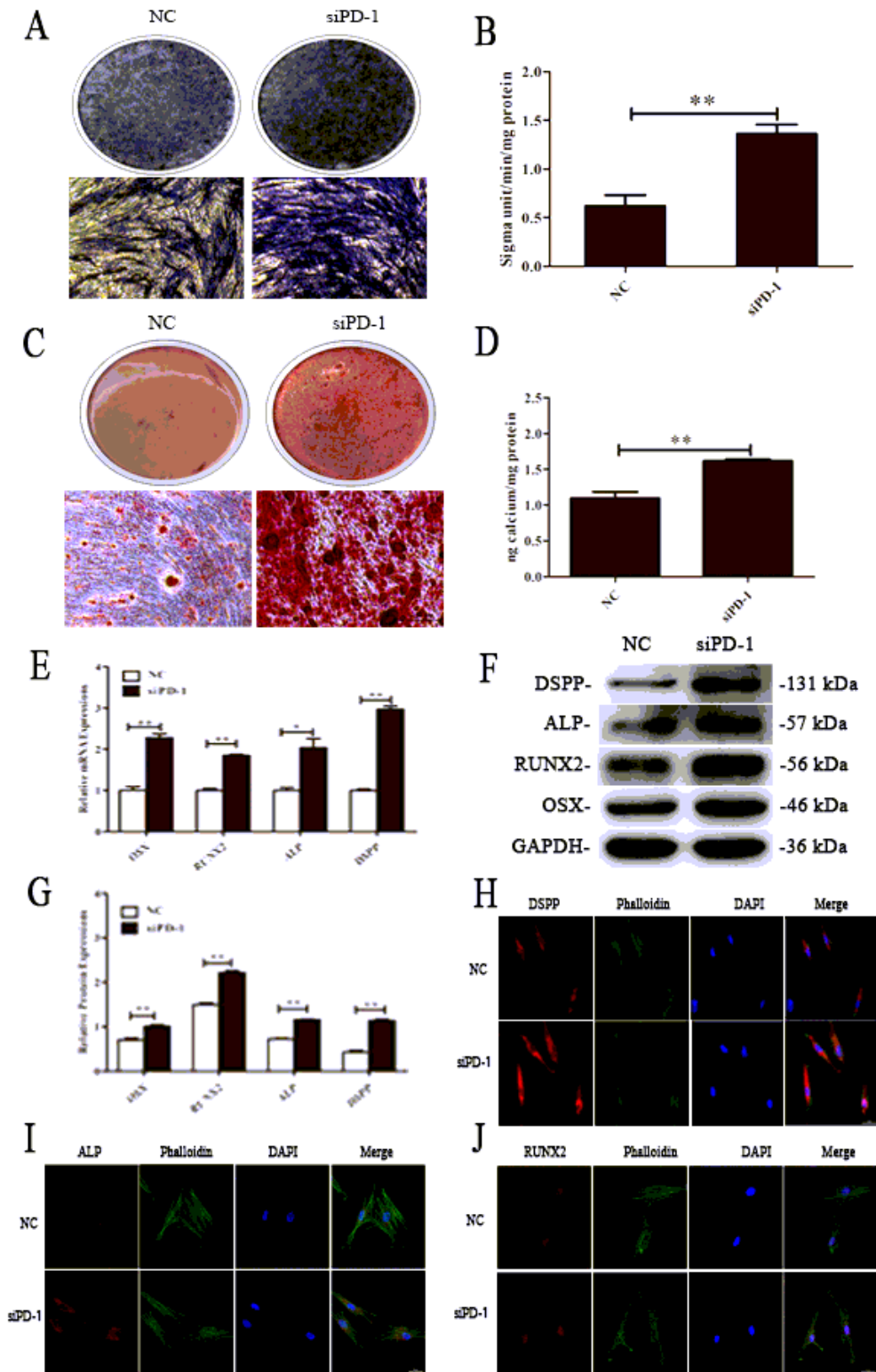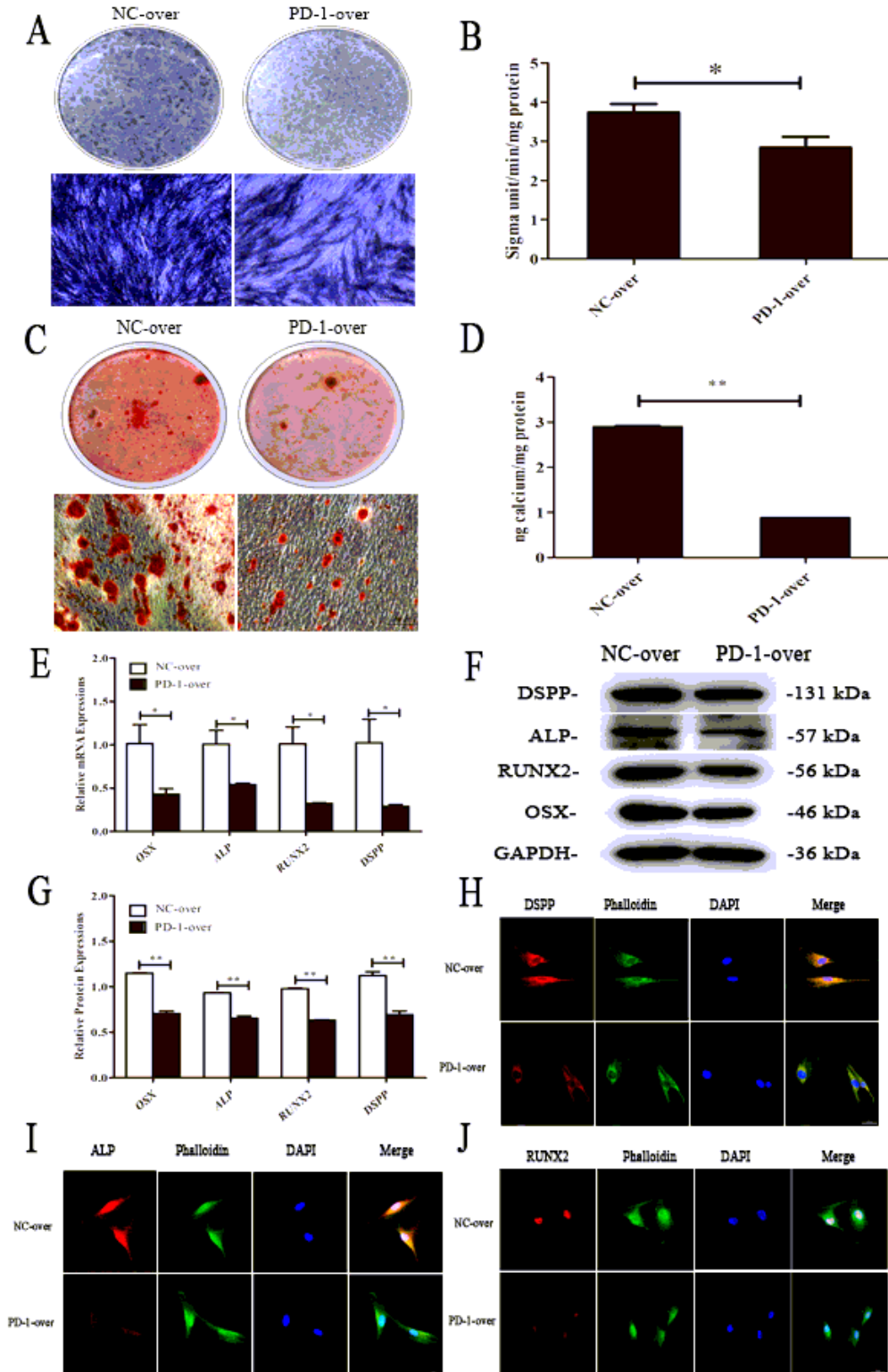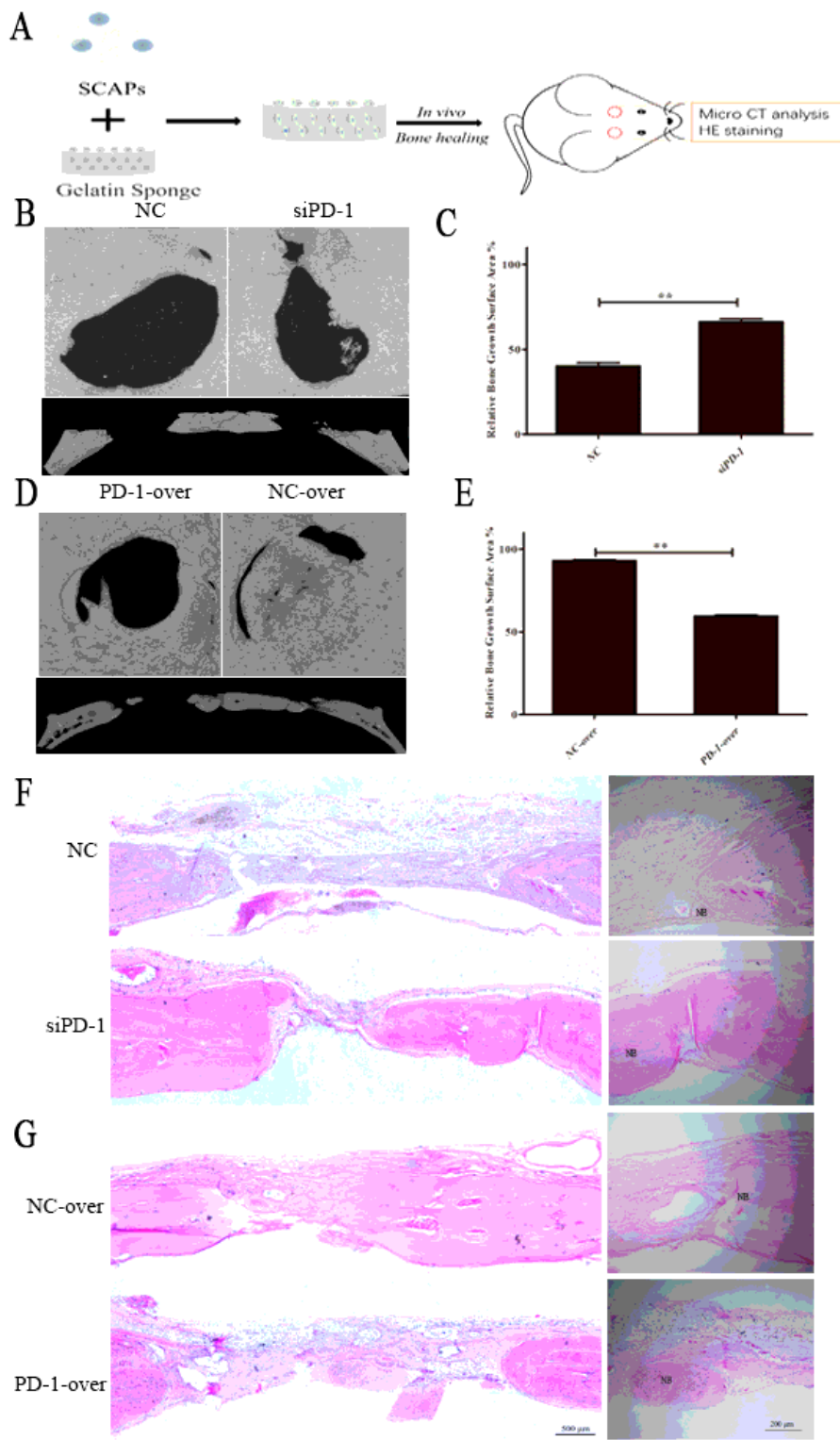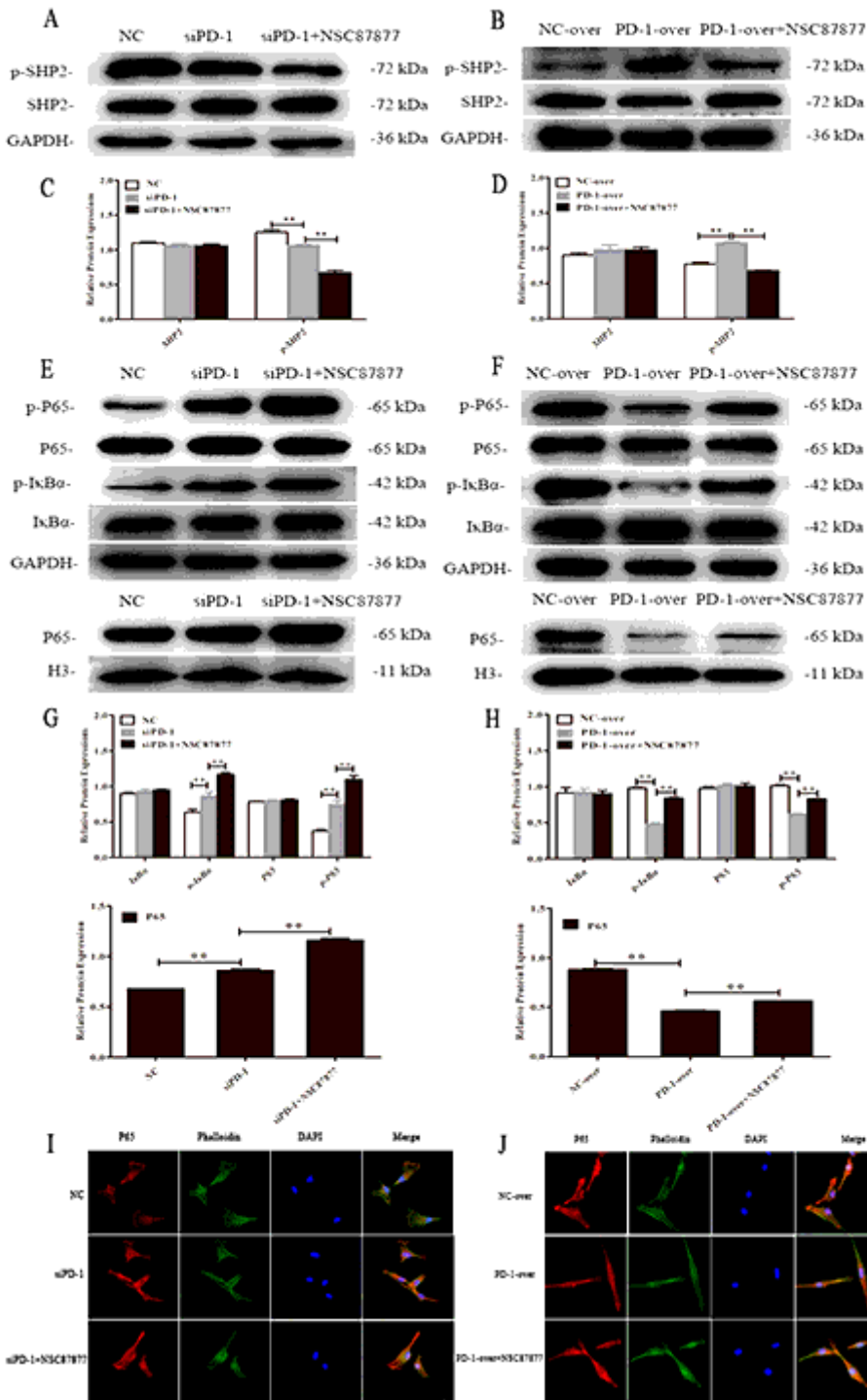
Figure 4

Downregulated PD-1 increased osteogenic and odontogenic differentiation of SCAPs (A) Images of ALP staining in NC group, si-PD-1 group for 7 days (scale bar=100 μm); (B) ALP activity assay was conducted when cells were cultured for 7 days (*p<0.05, **p<0.01); (C) Images of ARS staining for mineralized matrix in NC, siPD-1 groups (scale bar=100 μm); (D) CPC assay were conducted to get quantification of ARS staining (*p<0.05, **p<0.01); (E) Expression levels of osteo/odontogenic related genes (DSPP,

RUNX2, ALP and OSX) were assessed by qRT-PCR (*p<0.05, **p<0.01); (F) Expressions of osteo/odontogenic markers (DSPP, RUNX2, ALP and OSX) were assessed by western blot; (G) The histogram shows the quantification of band intensities (*p<0.05, **p<0.01); (H) Immunofluorescence detection indicated that downregulated PD-1 increased the protein expression of DSPP (scale bar=50 μm); (I) The protein expression of ALP was determined by immunofluorescence assay (scale bar=50 μm); (J) The protein expression of RUNX2 was assessed by immunofluorescence detection (scale bar=50 μm).

Figure 5

Upregulated PD-1 suppressed osteogenic and odontogenic differentiation of SCAPs (A) Images of ALP staining in NC-over, PD-1-over for 7 days. (B) Relative ALP activity on day 7. (*p<0.05, **p<0.01); (C) Results of ARS staining on day 14. (D) Relative quantitative analysis of ARS staining (*p<0.05, **p<0.01); (E) Relative mRNA expression of osteo/odontogenic genes (DSPP, RUNX2, ALP, and OSX) (*p<0.05, **p<0.01). (F) Western blot analysis of osteogenic and odontogenic markers in SCAPs; (G) Relative quantitative analysis of protein bands for DSPP, RUNX2, ALP, and OSX (*p<0.05, **p<0.01); (H) Immunofluorescence detection indicated that upregulated PD-1 decreased the protein expression of DSPP (scale bar=50µm). (I) Immunofluorescence detection indicated that PD-1 overexpression decreased the protein expression of ALP (scale bar=50 µm); (J) Immunofluorescence detection indicated that upregulated PD-1 decreased the protein expression of RUNX2 (scale bar=50 µm).

Figure 6

PD-1inhibited bone healing in a rat calvarial bone defects model (A) SCAPs with PD-1 overexpression or PD-1 knockdown were used in a rat calvarial bone defects model. The effect was confirmed by radiographic and histological analysis. (B) The results of micro-CT analyses in siPD-1 group and NC group; (C) The histogram shows the quantification of the area of newly formed bone in (B) (*p<0.05, **p<0.01); (D) The results of micro-CT analyses in PD-1-over group and NC-over group; (E) The histogram

shows the quantification of the area of newly formed bone in (D) (*p<0.05, **p<0.01). (G) HE staining in coronal images of bone defects in the NC group and siPD-1 group after 12 weeks. (H) HE staining in coronal images of bone defects in the NC-over group and PD-1-over group after 12 weeks. NB represents the newly formed bone.

Figure 7

Knockdown of PD-1 suppressed the phosphorylation of SHP2; overexpression of PD-1 promoted the phosphorylation of SHP2 (A) Western blot analysis of SHP2 signal related markers in SCAPs (NC group, siPD-1 group, siPD-1+NSC87877 group); (B) Western blot analysis of SHP2 signal related markers in

SCAPs (NC-over group, PD-1-over group, PD-1-over+NSC87877 group); (C) Relative quantitative analysis of band intensities: p-SHP2, SHP2 in (A) (*p<0.05, **p<0.01); (D) Relative quantitative analysis of band intensities: p-SHP2, SHP2 in (B) (*p<0.05, **p<0.01); (E) Western blot analysis of NF-κB signal related markers in SCAPs (NC group, siPD-1 group, siPD-1+NSC87877 group); (F) Western blot analysis of NF-κB signal related markers in SCAPs (NC-over group, PD-1-over group, PD-1-over+NSC87877 group); (G) Relative quantitative analysis of band intensities: p-P65, P65, p-IκBα, IκBα and nuclear P65 in (E) (*p<0.05, **p<0.01); (H) Relative quantitative analysis of band intensities: p-P65, P65, p-IκBα, IκBα and nuclear P65 in (F) (*p<0.05, **p<0.01); (I) Immunofluorescence detection indicated that PD-1 knockdown decreased the protein expression of nuclear P65, but NSC87877 increased the protein expression of nuclear P65 (scale bar=50 μm); (J) Immunofluorescence detection indicated that PD-1 overexpression increased the protein expression of nuclear P65, but NSC87877 decreased the protein expression of nuclear P65 (scale bar=50 μm).
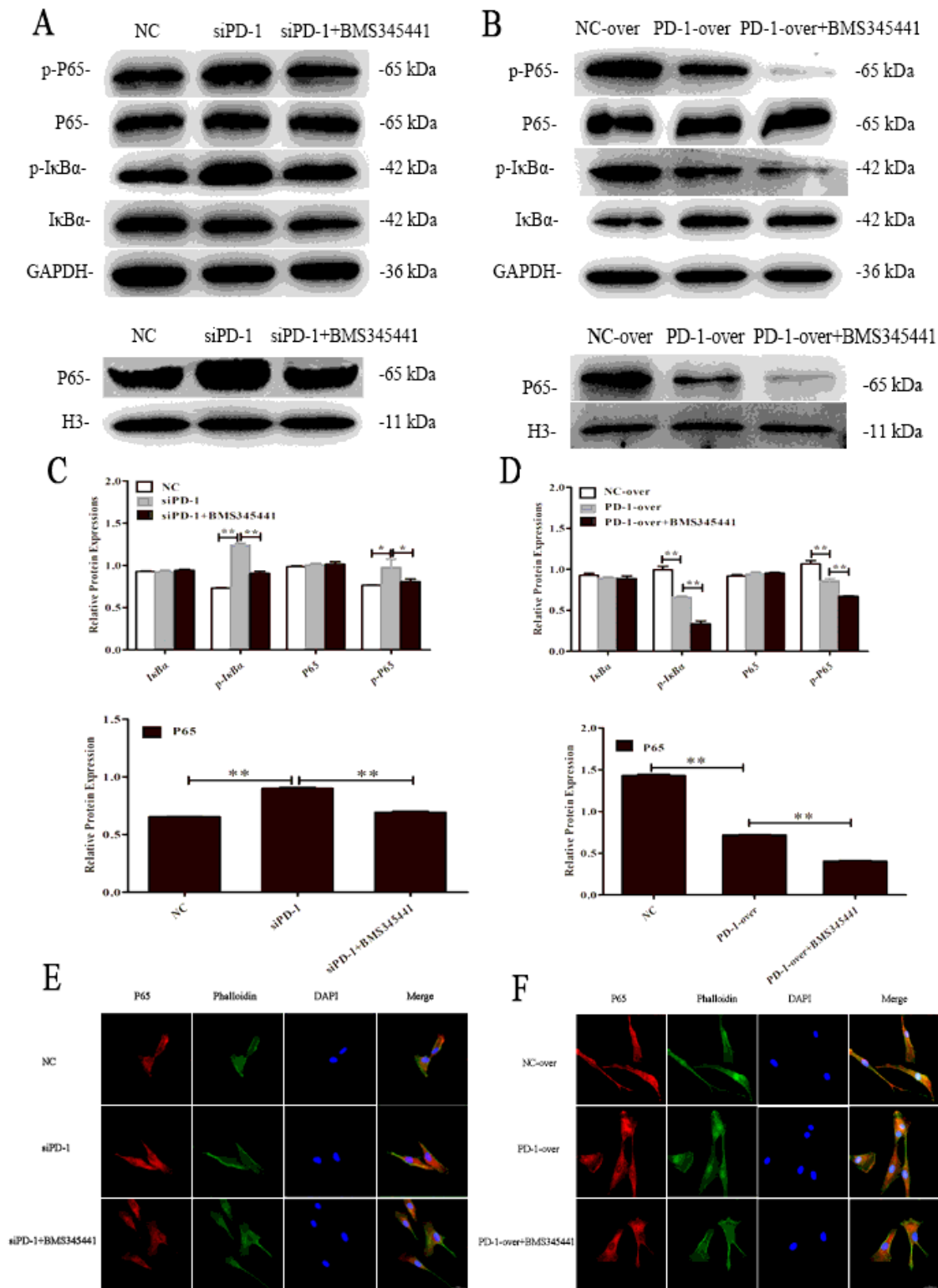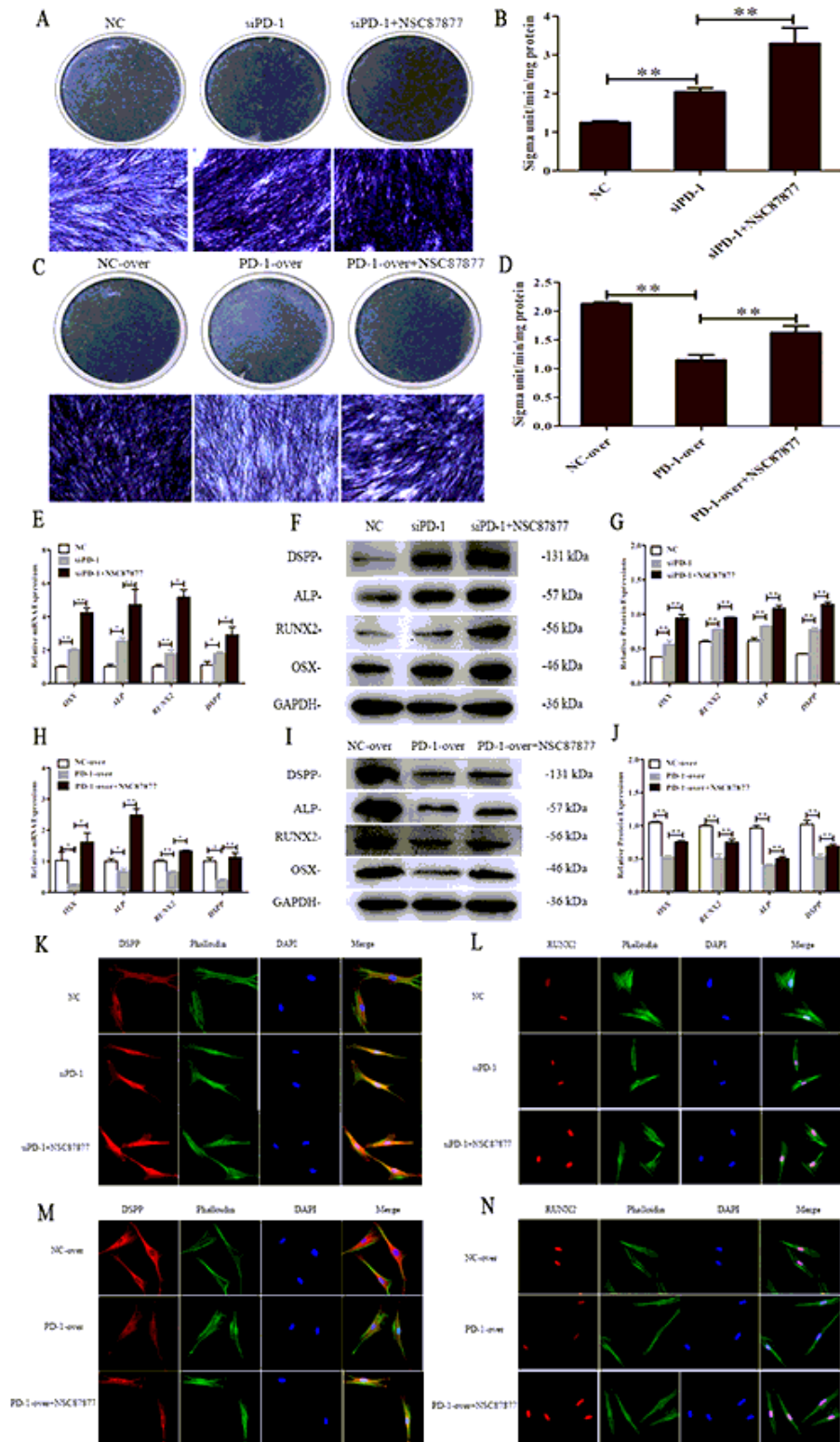
Figure 8

Knockdown of PD-1 activated NF-κB signal; overexpression of PD-1 suppressed NF-κB signal (A) Western blot analysis of NF-κB signal related markers in SCAPs (NC group, siPD-1 group, siPD-1+BMS345441 group); (B) Western blot analysis of NF-κB signal related markers in SCAPs (NC-over group, PD-1-over group, PD-1-over+BMS345441 group); (C) Relative quantitative analysis of band intensities: p-P65, P65, p-IκBα, IκBα and nuclear P65 in (A) (*p<0.05, **p<0.01); (D) Relative quantitative analysis of band

intensities: p-P65, P65, p-IκBα, IκBα and nuclear P65 in (B) (*p<0.05, **p<0.01); (E) Immunofluorescence detection indicated that PD-1 knockdown decreased the protein expression of nuclear P65, and BMS345441 reduced the protein expression of nuclear P65 (scale bar=50 μm); (F) Immunofluorescence detection indicated that PD-1 overexpression increased the protein expression of nuclear P65, but BMS345441 decreased the protein expression of nuclear P65 (scale bar=50 μm).
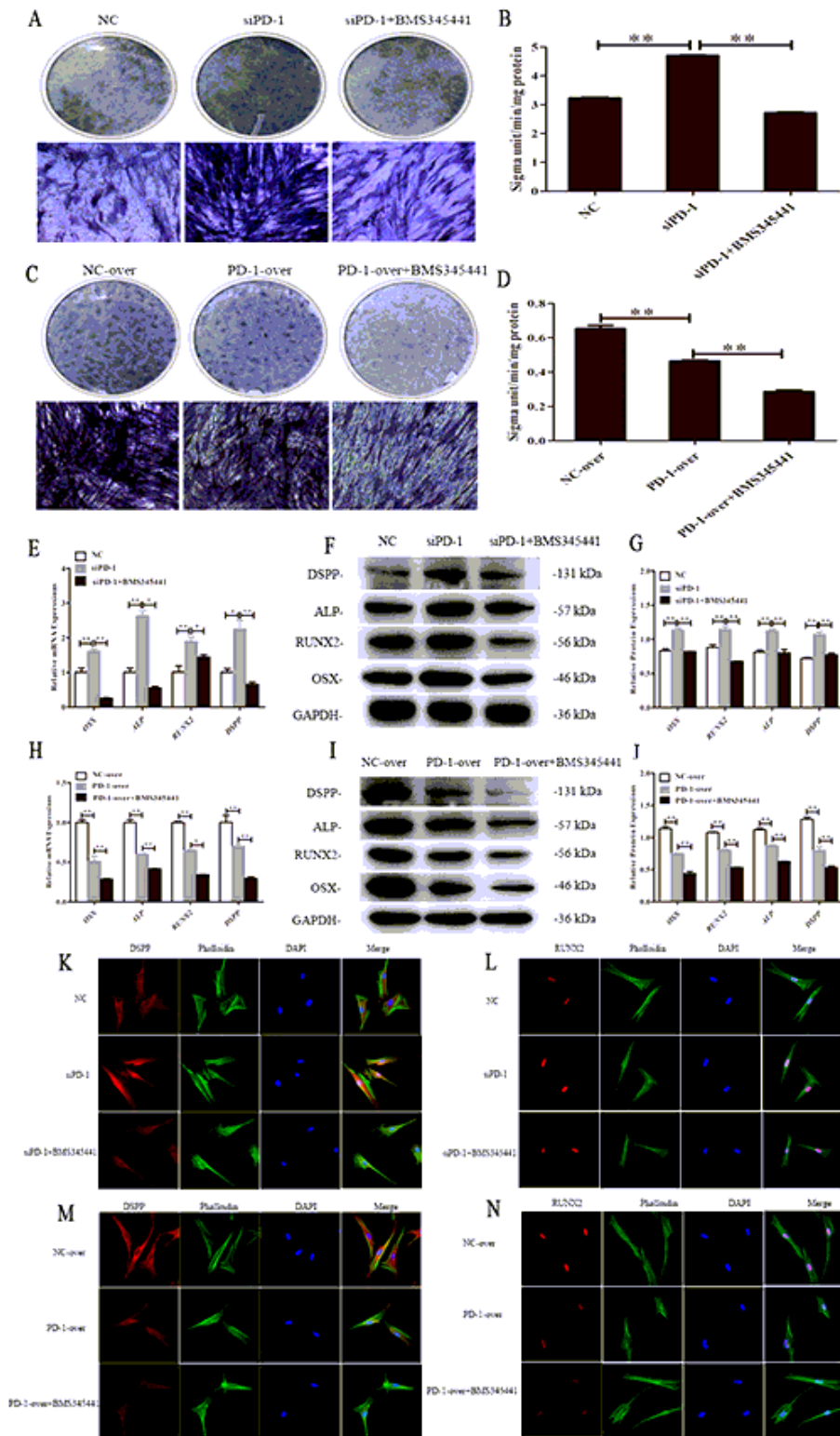

Figure 9

Inhibition of SHP2 signaling pathway promoted downregulated PD-1-enhanced osteogenic and odontogenic differentiation of SCAPs; Inhibition of SHP2 signaling pathway promoted upregulated PD-1-inhibited osteogenic and odontogenic differentiation of SCAPs (A) Images of ALP staining in NC group, siPD-1 group, siPD-1+NSC87877 group (scale bar=50 μm); (B) ALP activity assay in NC group, siPD-1 group, siPD-1+NSC87877 group (*p<0.05, **p<0.01); (C) Images of ALP staining in NC-over group, PD-1-over group, PD-1-over+NSC87877 group (scale bar=100 μm); (D) ALP activity assay in NC-over group, PD-1-over group, PD-1-over+NSC87877 group (*p<0.05, **p<0.01); (E) QRT-PCR analysis of osteogenic and odontogenic markers in SCAPs (NC group, siPD-1 group, siPD-1+NSC87877 group) (*p<0.05, **p<0.01); (F) Western blot analysis of osteogenic and odontogenic markers in SCAPs (NC group, siPD-1 group, siPD-1+NSC87877 group) (*p<0.05, **p<0.01); (G) Relative quantitative analysis of the corresponding protein band for DSPP, RUNX2, ALP, and OSX (*p<0.05, **p<0.01); (H) QRT-PCR analysis of osteogenic and odontogenic markers in SCAPs (NC-over group, PD-1-over group, PD-1-over+NSC87877 group) (*p<0.05, **p<0.01); (I) Western blot analysis of osteogenic and odontogenic markers in SCAPs (NC-over group, PD-1-over group, PD-1-over+NSC87877 group); (J) Relative quantitative analysis of the corresponding protein band for DSPP, RUNX2, ALP, and OSX (*p<0.05, **p<0.01); (K) Immunofluorescence detection indicated that PD-1 knockdown enhanced the protein expression of DSPP, and NSC87877 increased the protein expression of DSPP (scale bar=50 μm); (L) Immunofluorescence detection indicated that PD-1 knockdown increased the protein expression of RUNX2, but NSC87877 promoted the protein expression of RUNX2 (scale bar=50 μm); (M) Immunofluorescence detection indicated that PD-1 overexpression reduced the protein expression of DSPP, and NSC87877 increased the protein expression of DSPP (scale bar=50 μm); (N) Immunofluorescence detection indicated that PD-1 overexpression decreased the protein expression of RUNX2, but NSC87877 promoted the protein expression of RUNX2 (scale bar=50 μm).
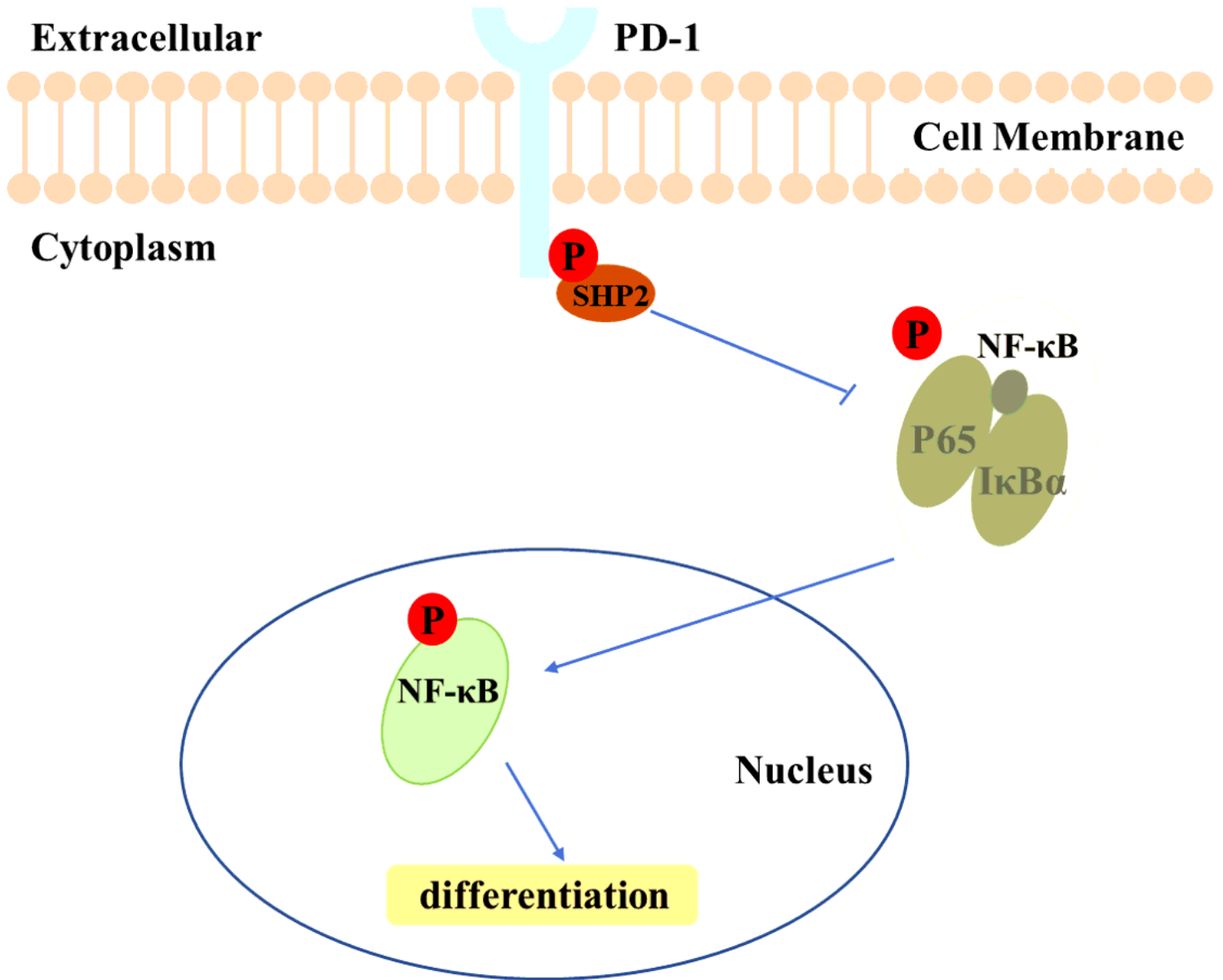
Figure 10

Inhibition of NF-κB signaling pathway inhibited downregulated PD-1-enhanced osteogenic and odontogenic differentiation of SCAPs; Inhibition of NF-κB signaling pathway inhibited PD-1 inhibited osteogenic and odontogenic differentiation of SCAPs (A) Images of ALP staining in NC group, siPD-1 group, siPD-1+ BMS345441 group (scale bar=50 μm); (B) ALP activity assay in NC group, siPD-1 group, siPD-1+ BMS345441 group (*p<0.05, **p<0.01); (C) Images of ALP staining in NC-over group, PD-1-over

group, PD-1-over+ BMS345441 group (scale bar=100 μm); (D) ALP activity assay in NC-over group, PD-1-over group, PD-1-over+ BMS345441 (*p<0.05, **p<0.01); (E) QRT-PCR analysis of osteogenic and odontogenic markers in SCAPs (NC group, siPD-1 group, siPD-1+ BMS345441 group) (*p<0.05, **p<0.01); (F) Western blot analysis of osteogenic and odontogenic markers in SCAPs (NC group, siPD-1 group, siPD-1+BMS345441 group) (*p<0.05, **p<0.01); (G) Relative quantitative analysis of the corresponding protein band for DSPP, RUNX2, ALP, and OSX (*p<0.05, **p<0.01); (H) QRT-PCR analysis of osteogenic and odontogenic markers in SCAPs (NC-over group, PD-1-over group, PD-1-over+ BMS345441) (*p<0.05, **p<0.01); (I) Western blot analysis of osteogenic and odontogenic markers in SCAPs (NC-over group, PD-1-over group, PD-1-over+ BMS345441) (*p<0.05, **p<0.01); (J) Relative quantitative analysis of the corresponding protein band for DSPP, RUNX2, ALP, and OSX (*p<0.05, **p<0.01); (K) Immunofluorescence detection indicated that PD-1 knockdown enhanced the protein expression of DSPP, and BMS345441 decreased the protein expression of DSPP (scale bar=50 μm); (L) Immunofluorescence detection indicated that PD-1 knockdown increased the protein expression of RUNX2, but BMS345441 reduced the protein expression of RUNX2 (scale bar=50 μm). (M) Immunofluorescence detection indicated that PD-1 knockdown enhanced the protein expression of DSPP, and BMS345441 decreased the protein expression of DSPP (scale bar=50 μm); (N) Immunofluorescence detection indicated that PD-1 knockdown increased the protein expression of RUNX2, but BMS345441 reduced the protein expression of RUNX2 (scale bar=50 μm).

Figure 11

Schematic diagram for PD-1/ SHP2 /NF-κB axis Schematic diagram for the activation of SHP2 and NF-κB pathways by PD-1 overexpression and inhibition. PD-1 overexpression can trigger the phosphorylation of SHP2, and suppress the phosphorylation of IκBα, which subsequently results in the rapid hydrolysis of IκBα. P65 is then phosphorylated and transported into nuclei, which finally causes the activation of NF-κB pathway.